sustainability

MDPI

Article

Buffer-Aided Relaying Strategies for Two-Way Wireless Networks

Vignon Fidele Adanvo [1], Samuel Mafra [1,*], Samuel Montejo-Sánchez [2], Evelio M. García Fernández [3] and Richard Demo Souza [4]

[1] National Institute of Telecommunications (INATEL), Santa Rita Sapucai 37540-000, MG, Brazil
[2] Programa Institucional de Fomento a la I+D+i, Universidad Tecnológica Metropolitana (UTEM), Santiago 8940577, Chile
[3] Department of Electrical Engineering, Federal University of Parana, Curitiba 81531-990, PR, Brazil
[4] Department of Electrical and Electronics Engineering, Federal University of Santa Catarina, Florianopolis 88040-900, SC, Brazil
* Correspondence: samuelbmafra@inatel.br

Abstract: The energy and time efficiency of wireless sensor networks (WSNs) is frequently affected by the low reliability of their links. To mitigate the outage probability, cooperation topologies are used. However, these topologies have particular challenges since the relay consumes energy in assisting a foreign communication, and the successful transmission in each direction is conditioned to the availability of the two segments involved in the communication. To overcome the temporary unavailability of a link, the use of buffers in the relay has been proposed, but energy and time efficiency remain a challenge for basic configurations. We propose two-way buffer-aided relaying strategies that exploit the presence of buffers in the different nodes that participate in the communication, as well as the efficient use of buffer capacity. The proposed strategies make the decision to forward the messages in one of the communication directions or broadcast coded messages based on buffer and channel state information. Firstly, we evaluate the impact of considering the use of buffers in the transmitter nodes. Then, we propose and evaluate the impact of the full and joint use of the entire buffer capacity to assist communication in both directions. Finally, we evaluate the performance of a system that exploits both the use of full and joint buffering and the presence of buffering in the transmitter. The results show that better performance, in terms of outage probability, is obtained by the third strategy; since it allows the buffer capacity to be exploited to a greater extent in the most urgent direction at each moment, as well as to select the start of each transmission to a viable communication opportunity. This represents a notable benefit in terms of energy and time efficiency for WSNs since unnecessary transmission of information is avoided, the number of idle slots decreases, and the amount of information per unit of time and energy increases.

Keywords: buffer; cooperative communication; machine type communication; Markov chain; outage probability; two-way relay network

check for updates

Citation: Adanvo, V.F.; Mafra, S.; Montejo-Sánchez, S.; Fernández, E.M.G.; Souza, R.D. Buffer-Aided Relaying Strategies for Two-Way Wireless Networks. *Sustainability* **2022**, *14*, 13829. https://doi.org/10.3390/su142113829

Academic Editor: Manuel Fernandez-Veiga

Received: 31 August 2022
Accepted: 9 October 2022
Published: 25 October 2022

Publisher's Note: MDPI stays neutral with regard to jurisdictional claims in published maps and institutional affiliations.

Copyright: © 2022 by the authors. Licensee MDPI, Basel, Switzerland. This article is an open access article distributed under the terms and conditions of the Creative Commons Attribution (CC BY) license (https://creativecommons.org/licenses/by/4.0/).

1. Introduction

Machine Type Communication (MTC) or Machine-to-Machine Communications (M2M) is an automated data communication where a series of devices or "things" are connected to the Internet or directly connected and communicate with each other with little or no human intervention. In recent years, it has been the subject of numerous investigations, mainly in 5G networks, due to the rapid growth in the number of devices connected [1]. Some applications of this communication are focused on the management of smart cities [2], while others are in industries [3] and in 6G [4]. Access control, resource allocation [5], massive access [6], and latency [7] are some of the most exploited topics of this technology in the scientific literature. In an MTC environment, devices are interconnected and exchange data with each other or with a server [8].

Specifically, the wireless sensor networks (WSN) are the base of the Internet of things (IoT) that all together give rise to the smart city [9]. These WSNs consist of several sensors, which are densely distributed to observe physical or environmental conditions, such as humidity, temperature, light intensity, CO_2, and gas concentration [9–11]. Undeniably, IoT evolution must prioritize the sustainability of future wireless networks, making them energy-efficient and environmentally friendly. Thus, the dynamic and efficient management of power resources is essential to offer a sustainable energy solution to meet the energy demands of these massive IoT networks [11]. In addition, in [12], the authors described green 5G/6G technologies and sustainability indicators. Some of the multiple profits of developing new agricultural technologies [13] and applications include the cost reduction around the building and deployment of them, together with more energy-efficient consumption [14,15]. On the other hand, in a smart city, a large number of smart sensors are operating and creating a large amount of data for a large number of applications, with challenging connectivity of the sensors to the data center through the communication network, which in turn requires expensive infrastructure [16]. Therefore, issues such as sustainability [9], autonomy [10], fault detection [14], and coverage [16] remain in the sights of researchers to increase the reliability and efficiency of these networks.

Various solutions have been proposed to mitigate the problems found in WSN, particularly M2M communication, such as the characteristics of the propagation medium, the hardware system, and the communication protocols. Some of these solutions propose sustainable cooperative communication (CC) through proposals based on wireless powered networks and energy harvesting [17]. The CC enables distributed nodes in a wireless network to collaborate, to realize a form of spatial diversity to combat the detrimental effects of fading [18]. Different cooperative techniques such as relays, distributed antenna systems, and multi-cell coordination were presented in [19]. In [20], the authors study the reliability and the energy efficiency provided by using the relays in a unilateral cooperative network. Furthermore, in [21], the authors show that using relays improves spectral efficiency through mathematical and simulated models. In contrast, in [22], the authors show through experimental methods that the use of relays can improve system performance in terms of system capacity.

In addition to unilateral CC, bidirectional CC is also found in the literature. Bidirectional CC allows two devices to exchange data in both directions for one or more relays; this paradigm is denoted a Two-Way Relay Network (TWRN) and has been exploited in [23]. The main opportunities and challenges of these systems are discussed in [24]. Some application examples of this form of transmission are satellite communications [25], cellular communications, [26] and wireless sensor networks [27]. In [28], the authors investigate the different transmission protocols in TWRN. Among the rules of these protocols are, for example, time-division broadcasting (TDBC) [29], physical-layer network coding (PNC) [28], or multiple access broadcasting [29]. Additionally, in [30], the authors show that, in general, for ideal wireless channel conditions, the TDBC protocol outperforms other transmission protocols. However, buffers have been introduced in cooperative communications as a technique to improve the performance of cooperative systems.

The use of buffers to temporarily store packets allows a node to explore the available information to make a decision (whether to receive, transmit, or receive and transmit). For example, within a frame, it may be that a link is not available to transmit a packet; in this case, using a buffer to store this packet can be beneficial. This benefit allows that a certain packet cannot be lost due to temporal channel unavailability. In [24], the authors show that the use of relay with buffer in a cooperative half-duplex relay network can significantly improve the system throughput and the outage probability (OP) compared to the existing conventional relay networks.

1.1. Related Work

Several authors explore the aforementioned topics through new proposals or global reviews of existing ones [31–44]. For example, in a one-way communication system, the authors in [31] carry out a Markovian analysis of a multiple access system (i.e., several source users sending information for a single destination) assisted by relay. The optimal number of users that maximizes the aggregate throughput was obtained analytically. However, this user number is conditioned by the characteristics of the link and the transmission probabilities. Nonetheless, to mitigate the energy constraints on the transmitters (i.e., the source and the relay), the authors in [32] study a conventional two-hop relay network under energy buffering of unlimited capacity. A Markovian analysis was carried out, where, in addition to the exact stable region of maximum yield, the closure of the inner and the outer bound was obtained, which turned out to be identical. Additionally, the authors in [33] propose two routing algorithms: effective energy and reliable delivery (EERD) and cooperative effective energy and reliable delivery (CoEERD), in order to mitigate such challenges of underwater wireless sensor networks. Specifically, the CoEERD manages to increase the system's reliability compared to the EERD at the cost of increasing energy consumption.

On the other hand, in a two-way communication system, the authors in [45] review and analyze various link selection protocols in buffer-assisted relay systems. Performance comparisons were made based on outage probability and average packet delay. The results demonstrated the superiority of buffer state information (BSI)-based selection methods in terms of OP. In [34,46], the authors investigate buffer-assisted TWRNs with fixed-rate transmission. The efficiency of the buffer used in the relay node in a TWRN for delay-tolerant [46] and non-tolerant [34] applications was verified. However, these proposals consider an infinite buffer size, making its implementation in current wireless communication systems unfeasible. In [35], the authors study the throughput and delay in full-duplex TWRN. The proposed adaptive protocol combines the states of the buffer, the link losses, and OP to decide to transmit, receive, or transmit and receive. Additionally, in [36], the authors perform an analysis based on multi-agent reinforcement learning to maximize the system throughput by considering the combination of buffer states and link states. Despite extensive research on buffers used in the literature, the use of independent buffers in each direction in a TWRN is always proposed, but the joint use of a single buffer in the relay is not exploited, nor is the impact of the use of buffers in the sources.

In order to improve the performance of cooperative buffering systems, several authors introduce network coding in the physical layer. PNC allows, at the medium access control (MAC) level, for two or more packets to be able to be combined before being sent [37], which was also implemented in a conventional TWRN in [38]. In contrast to the conventional TWRN model [38], in [39], the authors show the benefits of a buffer-assisted TWRN where packets are XOR encoded before broadcasting the messages. In addition, in [40,47], the authors carry out exhaustive research work on the importance of coding the message before transmitting it with different transmission protocols. In [47], an improved transmission scheduling is used in which a finite buffer of the relay, signaling overhead, and link losses are jointly considered in a network coding scheme. This strategy improved transmission efficiency and avoided buffer overflow compared to existing conventional methods. On the other hand, in [40], the bit layer network coding (BNC) protocol is implemented in a proposal based on a Markov model where a reasonable buffer size can be configured to compromise performance and queue delay. This approach managed to increase throughput and decrease energy consumption compared to [47]. Additionally, in [41], the authors use BSI and channel state information (CSI) to propose a protocol based on a selective transmission scheme with Markov chain states in the relay. Better performance was obtained in this proposal compared to the one obtained in [40,47]. However, in the proposed schemes of [39–41,47], no strategy is observed to make the most of the buffer capacity, so considering it would allow us to carry out a comparative analysis.

To overcome the limitations of [41], the authors in [42] propose an MAC scheme for TWRN with several helpers. This proposal integrates a new cooperative retransmission technique based on bidirectional network coding with helpers. Better performance was obtained in terms of throughput than the cooperative relay model in TWRN, always for the asymmetric network. In addition, helpers can contribute to packet forwarding. Unlike [41], in [43], the impact of packet delays was analyzed in a buffer-assisted TWRN considering buffer and link delays. The minimum buffer size needed to optimize performance in terms of outage probability and mean packet delay was determined. However, this proposal does not provide for a high rate of transmission. To overcome this limitation, in [44], the Non-Orthogonal Multiple Access (NOMA) paradigm in buffer-assisted TWRN, with Time-division duplex (TDD) transmission protocol, was exploited. Better results are obtained mainly in the transmission rate compared to models [41–43].

However, these proposals do not limit the delay packets, a fundamental requirement to guarantee QoS in real-time silent multimedia transmission systems. Therefore, Ref. [48] proposes a buffer-assisted transmission with QoS reconfirmation under the constraint of QoS statistics using an adaptive link to allocate powers. This proposal manages to maximize the effective capacity of the system, in addition to providing a beneficial result for a transmission that is not limited by a certain delay. To complement the results obtained in [48], the authors in [49] investigate an IoT communication network in which, different from [48], the analysis is made under QoS constraints of end-to-end delay in terms of the maximum acceptable outage probability per delay. Furthermore, different optimization-based approaches (i.e., link scheduling and power allocation) were used for energy-efficient adaptive resource allocation. Despite these achievements, it would be essential to evaluate the possibility of incorporating an algorithm that would allow exploiting, in addition to network coding, a strategy that explores the total capacity of the buffer at different transmission time slots.

1.2. Motivation and Contributions

Motivated by the system performance of the previous research works considering TWRNs and the benefits of using buffers on devices [8,24,41–43,48–50], we develop and investigate different buffer strategies in TWRNs. This approach can be improved if some of the link selection protocols presented in [45] were implemented. However, in this work, we limit ourselves to the worst case, which is when only one relay is available, to illustrate the impact of using the buffer through different strategies. One of the proposals made in this document, based on what was presented in [39,47], considers for the first time a novel algorithm capable of increasing the number of packets transmitted per time slot. In addition, a new buffering strategy is proposed that makes it possible to take advantage of the buffer capacity providing a low outage probability. We also validate our proposals through analytical and simulation results by comparing them with existing models. Consequently, the contributions of this work are as follows:

- Based on the models presented in [39,47], we proposed an innovative transmission strategy in addition to network coding, which allows for a lower outage probability and better utilization of buffer capacity.
- We propose the use of buffers in all the system nodes to increase the number of decision-making options in terms of the efficient use of channel spectral resources. This proposal surpasses existing models because of the inclusion of buffers in the source devices since they can exploit this resource as long as the transmission channels are not available.
- In order to increase the efficient use of the memory capacity available in the relay, we propose the full and joint use of a single buffer to assist communication in both directions, which allowed us to fully exploit the memory capacity to increase the performance of the system.

- Finally, we propose a rule-based algorithm capable of making better use of the spectrum available for each frame, which exceeds the existing models in terms of the number of packets received successfully, according to the results obtained.

In a nutshell, Table 1 shows the main features of the related works and our proposals.

Table 1. Main features of the related works and our proposals.

References and Proposals	Feature						
	Transmission Protocol	Single Buffer	Source Buffer	Finite Buffer	Network Coding	BSI	CSI
[28]	TDBC, PNC and OSS	x	x	x	x	x	x
[35]	FD-TWRN	x	x	x	✓	x	x
[39]	PNC	x	x	✓	✓	✓	x
[40]	BNC	x	x	✓	✓	x	✓
[41]	Hybrid	x	x	✓	✓	✓	✓
[42]	TDMA	x	x	✓	✓	✓	x
[43]	XORed	x	x	✓	✓	✓	x
[44]	TDD	x	x	x	x	x	x
[47]	XOR-TWRN	x	x	✓	✓	✓	x
Our scheme with a single buffer in the relay.	TDBC and XOR	✓	x	✓	✓	✓	✓
Our scheme with two separate buffers in the relay and source.	TDBC and XOR	x	✓	✓	✓	✓	✓
Our scheme with a single buffer in the relay and buffer in the source.	TDBC and XOR	✓	✓	✓	✓	✓	✓

The rest of this paper is organized as follows: first, in Section 2, the system model is presented. Then, in Section 3, the decision rules and the transmission algorithm are described. Additionally, in Section 4, the mathematical analysis for the cases with/without buffer is presented. Next, the simulations and the numerical results are given in Section 5. Finally, the conclusions are presented in Section 6. The abbreviations used in this paper are summarized in the back matter, while the symbols are summarized in Table 2.

Table 2. List of symbols.

Symbol	Meaning
$\rightarrow$	Unilateral channel
$\rightleftharpoons$	Symmetrical channel
α	Path loss factor
B_{S_1} | B_{S_2}	Buffer of node S_1 | S_2
B_{S_1R} | B_{S_2R}	Relay buffer of S_1 to R | S_2 to R
B_{SR}	Relay buffer of S_1 to R and S_2 to R
d_{ij}	Distance between device i and j
γ_{ij}	Signal-to-noise ratio (SNR) between device i and j
h_{ij}	Channel response between nodes i and j
I_{ij}	Mutual information between device i and j
K_S | $\overline{K_S}$	The source buffer associated with the link available | unavailable
K_R	The relay buffer associated with the link available
λ_{ij}	The channel average power gain between device i and j
L | N	The maximum size buffers | single buffers
NP | $\overline{NP}$	Package generated in an available link | unavailable link
$\mathcal{O}_{ij}$	Probability of link outage between nodes i and j
ψ_R | ψ_T	Packet number to be received | transmitted

Table 2. *Cont.*

Symbol	Meaning
P_i	Transmit power in the device i
$Q_T \mid Q_R$	Relay buffer state suitable for transmit | receive
Q_{TR}	Relay buffer state suitable for transmit and receive
ρ_i	Signal-to-noise ratio measured by the transmitter i
r_i	Target transmission rate in the device i
SP	Stored packet
$v_{S_1} \mid v_{S_2}$	Number of packets in B_{SR} of $S_1 \mid S_2$
v_e	The number of packets corresponding to the link available in B_{SR}
	Lost packet
	Packet sent with success
R	Packet stored in the buffer of the relay
S	Packet stored in the source buffer

2. System Model

We consider a Two-Way Relay system that can have buffers in all nodes as shown in Figure 1. The network is composed of three nodes: the sources S_1, S_2 and the relay R. It is assumed that there is no direct link between S_1 and S_2 [51]; then, the nodes S_1 and S_2 communicate with each other via the relay node R. All nodes are equipped with an omnidirectional antenna and R operates in half-duplex mode with the decode-and-forward protocol [52]. All the channels involved are independent and identically distributed (iid) with non-frequency-selective Rayleigh-block fading and additive white Gaussian noise (AWGN). We also consider the channels to be symmetrical. The channel response between transmitter i and receiver j is denoted h_{ij} where $\{ij\} \subset \{S_1, S_2, R\} \mid i \neq j$. The channel average power gain is given by $\lambda_{ij} = d_{ij}^{-\alpha}$, where α is the path loss exponent, and d_{ij} is the distance normalized with respect to the distance between S_1 and S_2, i.e., $d_{S_1S_2} = 1$. Since we use a normalized distance with reference to S_1 and S_2, the relay will be positioned in an open interval of 0 and 1.

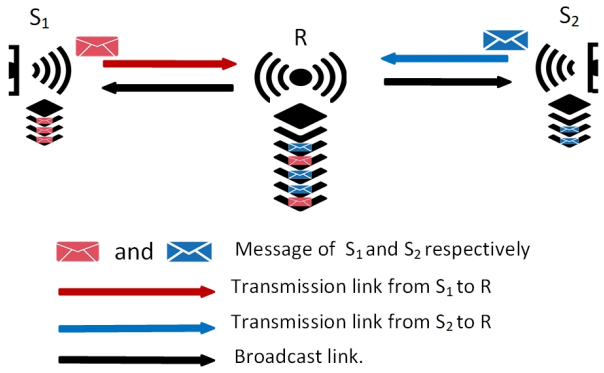


Figure 1. Two-way network with buffer implementation in all nodes.

Let B_{S_1} and B_{S_2} denote the buffers of nodes S_1 and S_2, respectively. The buffer of the relay has two configurations: the first configuration consists of two separate buffers for each direction denoted B_{S_1R} and B_{S_2R}, while the second configuration consists of implementing a single buffer for both directions denoted by B_{SR}. This last unexplored buffer configuration in the literature allows us to explore the full buffer capacity further, providing better results. In the first configuration, each buffer has size L, while in the second configuration, the single buffer has size $N = 2L$ to handle the two streams. The single buffer is twice the size of the separate buffers but can be used interchangeably to store packets traveling in one direction or the other. The use of a buffer in the devices provides a benefit in terms of the retention of the data transmitted in unfavorable channel conditions. Thus, it is assumed that this benefit increases with increasing buffer size. To simplify the analysis, it is assumed

that each unit of memory in the buffers is equivalent to the size of the packets. The target transmission rate is r_i in bits per channel use (bpcu).

Transmission takes place in three sub-time slots according to the TDBC protocol [29]—a priori, being two sub-time slots for the transmission of packets from the sources to the relay and one sub-time slot for their diffusion as summarized in Figure 2. However, this optimistic setting is only valid if successful transmissions on both channels are possible.

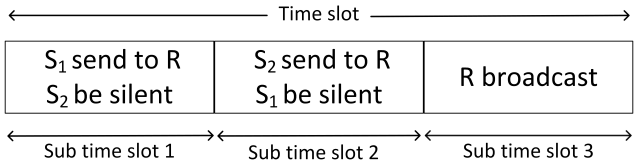


Figure 2. Time slot structure.

Note that a time slot is a minimum time required for each source to send a packet to the other, while a sub-time slot is a time needed for one of the sources to send a packet to the relay or for the relay to send or broadcast a packet. Network coding, i.e., exclusive OR (XOR), is used to combine in the relay and broadcast packets from both devices only when both links, $S_1 \rightleftharpoons R$ and $S_2 \rightleftharpoons R$ are available [53]. For example, if S_1 sends x_1 in the first sub-time slot and S_2 sends x_2 in the second, relay broadcasts messages x_1 and x_2 in the third sub-time slot through network coding. Each device can decode the received message without additional time, having the previous information of its message. This coding allows us to reduce the number of required slots from four to three originally. It is assumed that, in each time slot, a new packet is generated by the transmitting nodes. In buffered scenarios, this sub-time slot-based setting can be conveniently reconfigured according to BSI and CSI [39,47]. CSI allows the transmissions to be adapted to the current channel conditions to achieve reliable communication at high transmission rates. CSI could be obtained at the beginning of each transmission by the relay through channel sensing methods [29], which means that, in each time slot, the current conditions of the channel are known by the relay, similar to [54]. We assume that, at the beginning of each time slot, each source sends a very short-duration reference signal to the relay, through which it evaluates the availability of both channels. Based on this information and BSI, the relay sends a scheduling signal for the three subsequent sub-time slots; then, each source knows when to transmit and when to receive. This signal must also be short enough to neglect the time and energy consumption of the signaling phase compared to the transmission of a packet. The minimum size of the buffers used in the proposed schemes was set to three for separate buffers and to six when using a single buffer to guarantee full exploitation of all three sub-time slots. This configuration ensures that up to three packets can be sent depending on the buffer state and the link state.

Mutual Information and Outage Probability

An outage event occurs when the capacity of a given channel is less than the transmission rate at which devices operate during the packet transmission. The signal-to-noise ratio (SNR) on each link can be computed as

$$\gamma_{ij} = \frac{|h_{ij}|^2 P_i}{P_n}, \tag{1}$$

where P_i is the transmit power with $i \in \{S_1, S_2, R\}$, $i \neq j$, and P_n is the noise power. Consequently, the corresponding mutual information is given by [55],

$$I_{ij} = \frac{1}{3} \log(1 + \gamma_{ij}). \tag{2}$$

It can be noticed that, by using the decode-and-forward principle in the relay, the effective transmission rate must be less than the smallest value of mutual information between the transmission and broadcasting phases. In each frame, the TDBC protocol requires three sub-time slots, which justifies the term 1/3 in (2). Then, the probability of link outage is expressed as

$$\mathcal{O}_{ij} = \mathcal{P}(I_{ij} < r_i) = 1 - e^{-\frac{P_n}{\lambda_{ij}} \frac{2^{3r_i}-1}{P_i}}. \quad (3)$$

3. Decision Rules and Transmission/Reception Algorithm

In this section, different scenarios are analyzed in terms of the presence/absence of buffers in the nodes, transmission modes according to BSI/CSI, and decision rules in the relay. Scenario 1 assumes an unbuffered scheme. Scenarios 2 and 3 consider schemes using buffers in the relays with two separate buffers (one for each transmission direction) in Scenario 2 and a single buffer (of joint use) in Scenario 3. Finally, Scenarios 4 and 5 consider the use of buffers in the transmitters (sources) and relay, two separate buffers being in the relay in Scenario 4 and a single buffer in the relay in Scenario 5. The five scenarios are detailed in Figure 3.

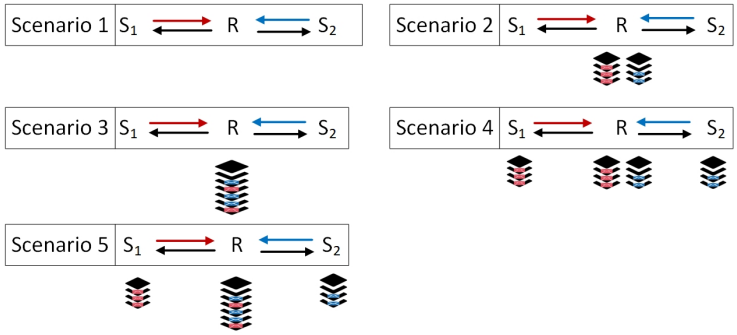


Figure 3. Five proposed scenarios that differ according to buffer usage.

The source generates a packet in each time slot that is transmitted, stored, or lost depending on the state of the buffer, the associated link, and the algorithm used. At the beginning of each transmission, whenever a packet is generated, and the link associated with this transmitter is available, then it is denoted NP, otherwise $\overline{NP}$ (which denotes the opposite of NP). In other words, if the link $S_1 \rightleftharpoons R$ is not available and the link $S_2 \rightleftharpoons R$ is available, then the new packet generated by S_1 is $\overline{NP}$ and the one generated by S_2 is NP. When NP and/or $\overline{NP}$ enter the queue, it is denoted SP (stored packet). Let ψ_T and ψ_R denote the number of packets to be transmitted and the number of packets to be received by the relay, respectively. For example, in a time slot, the relay can send two packets and receive one; in this case, $\psi_T = 2$ and $\psi_R = 1$. Decision rules are modeled according to the algorithm that increments the number of received packets. In the following subsection, the modeling of each analyzed scenario is described.

3.1. Scenario 1: No Buffer in Any Node

The method used to model Scenario 1 is shown in this subsection. Nodes are configured without buffers, and when at least one link is unavailable, an outage event occurs. The present scenario is analyzed in different articles, as in [29]. We consider this scenario as a benchmark for our analysis. Figure 4 shows the transmission scheme of Scenario 1 that models all the packets available for sending. In this figure, all valid possibilities to model the total number of packets in Scenario 1 are shown. For example, the packets are sent successfully if the two links are available.

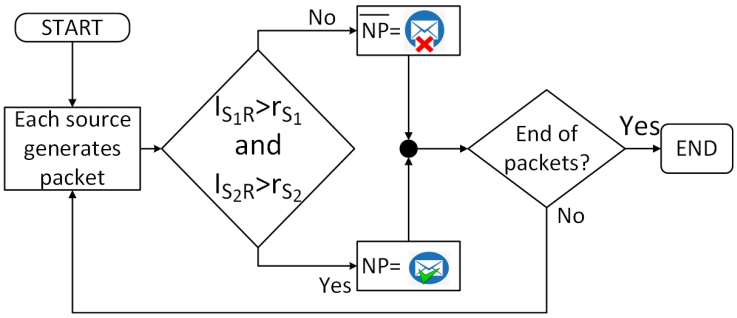


Figure 4. Scenario 1: No buffer on devices.

3.2. Scenario 2: Two Separate Buffers in the Relay Node

Due to the benefits provided by the use of buffers in the relay, the authors in [39,47] propose a system model of a bidirectional cooperative network based on BSI/CSI. A better performance was found in terms of throughput and OP. Furthermore, a balance was found between the buffer size and the delay caused. In this subsection, the technique used to model Scenario 2 is shown in order to compare with the proposed scenarios.

Let Q_T and Q_R denote the state of the buffer of the relay ready to transmit and the state of the buffer of the relay ready to receive, respectively. For example, if only link $S_1 \rightleftharpoons R$ is available, then the buffer ready to receive is B_{S_1R}, and the buffer ready to transmit is B_{S_2R}. Otherwise, the buffer ready to receive is B_{S_2R} and the buffer ready to transmit B_{S_1R}. To simplify that, we denote it Q_T and Q_R for both cases. Figure 5 shows the flowchart used to model all the valid possibilities for this scenario. In this figure, a packet is generated in each time slot. Note that, when the mutual information (I_{S_1R} and I_{S_2R}) of the two channels is less than r, then the generated packets are lost, and the cycle restarts whenever there are more packets available to be sent. Now, if the mutual information of one of the two channels is less than r, then the new packet generated on the unavailable link ($\overline{NP}$) is lost. In contrast, the one generated on the available link (NP) is stored in the buffer Q_R whenever Q_R is not full. The Q_T can transmit a number of packets equal to the minimum between three and the state of the referred buffer when $Q_R = L$ or equal to the minimum between two and the state of the referred buffer when $Q_R \neq L$. These processes are repeated until the end of the transmission. Generally, using BSI and CSI, the relay sends a reference signal to the transmitters as mentioned in Section 2. In addition, it contains the order of transmission of the nodes. This signal generates the following three decision possibilities in the nodes:

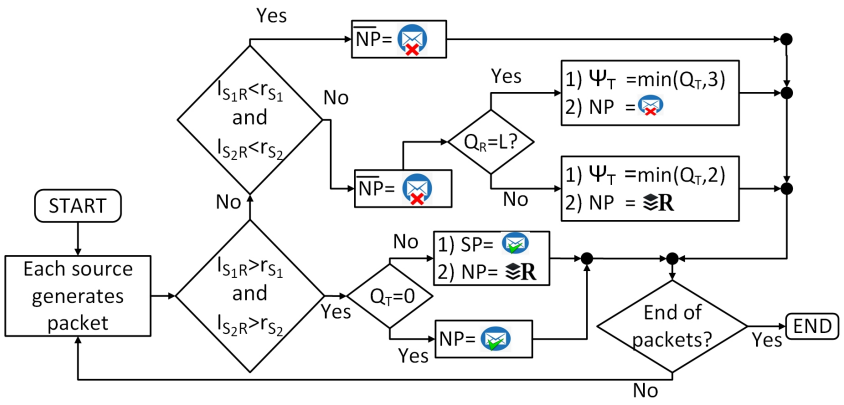


Figure 5. Scenario 2: Separate buffers on relay node.

- If both links are not available, both the packet from node S_1 and node S_2 are lost.
- If both links are available, the packet from S_1 is successfully sent to the destination or is stored in R according to the state of the buffer. When the buffers of the relay are full, then broadcast has priority. Similar events occur regarding the packet from S_2:

- If one of the links is available and the other is unavailable, two events occur:
  - On the available link, the node sends the packet to the relay when the associated buffer is not full; otherwise, it is lost.
  - On the unavailable link, the packet generated by the sender is lost. Packets in the buffer of the relay are sent.

Packets are serviced according to the First-In, First-Out (FIFO) protocol. For example, if all links are available and $Q_R = L$ where L is the maximum buffer capacity, the relay transmits first, then S_1 transmits to R, and S_2 transmits to R last. The order of transmission is dictated by the relay.

The proposed algorithms are used when only one of the symmetric channels is available, making the relay communicate with only one transceiver. For example, given the case where the link $S_1 \rightleftharpoons R$ is available and the link $S_2 \rightleftharpoons R$ is unavailable, then the relay only communicates with the transmitter S_1. Algorithm 1 shows the strategy used to increase the number of transmissions/receptions in the relay per time slot in this scenario. An illustrative example of the use of this algorithm follows: if the link $S_1 \rightleftharpoons R$ is available, and $S_2 \rightleftharpoons R$ is unavailable, and in addition, the state of buffer ready to receive is full, then this algorithm allows for transmitting and receiving a maximum of three packets stored in the relay and/or generated by the transmitter. In the same condition as CSI/BSI defined above, conventional buffer-assisted TWRN models can transmit a total of one packet in this time slot. Unlike the proposals in [39,47], using this algorithm, it is possible to increase the number of packets sent per time slot. However, when both links are available, the best transmission option is by network coding, i.e., exclusive OR [56].In other words, a diversity gain is achieved when the relay broadcasts the encoded information at the same sub-time slot. The algorithms used have a negligible computational cost because it is a simple condition-based (validation condition) that does not require a loop.

Algorithm 1 Scenario 2 transmission algorithm

Input Q_T, Q_R, L
$n_1 \leftarrow 3$
$n_2 \leftarrow 2$
if $Q_R = L$ **then**
    $\psi_T \leftarrow \min(n_1, Q_T)$
else
    $\psi_T \leftarrow \min(n_2, Q_T)$
    $\psi_R \leftarrow 1$
end if
Output ψ_T, ψ_R

3.3. Scenario 3: Single Buffer in the Relay Node

In Scenario 3, we present a new proposal to explore buffer capacity through a simple buffer strategy. In this scenario, the relay has a single buffer for both transmissions, unlike the previous one with separate buffers. This scenario is designed for an even more critical channel condition, where storage capacity can be increased without adding new resources to the system. In the case of using a single buffer in the relay, the packets stored in the buffer B_{SR} must be coordinated, always respecting the output order. The protocol for answering packets in the buffer implemented is FIFO, which means that the first packet that enters the buffer is the first one that leaves it. Thus, Q_{TR} is the state of the relay single buffer ready to transmit and receive.

Let v_{S_1}, v_{S_2} and v_e denote the number of packets destined to S_1 in B_{SR}, the number of packets destined to S_2 in B_{SR}, and the number of packets in the buffer B_{SR} destined to the receiver with the link unavailable, respectively. For example, in a time slot, if $S_1 \rightleftharpoons R$ is available, $S_2 \rightleftharpoons R$ is unavailable, and $Q_{TR} = 5$ being three packets destined for S_1 and two destined for S_2, then $v_{S_1} = 3$, $v_{S_2} = 2$, and $v_e = 2$. Figure 6 shows the strategy and

method used to model all the possibilities in this scenario. Based on BSI/CSI, the relay sends a reference signal to the transmitters and three possibilities can happen:

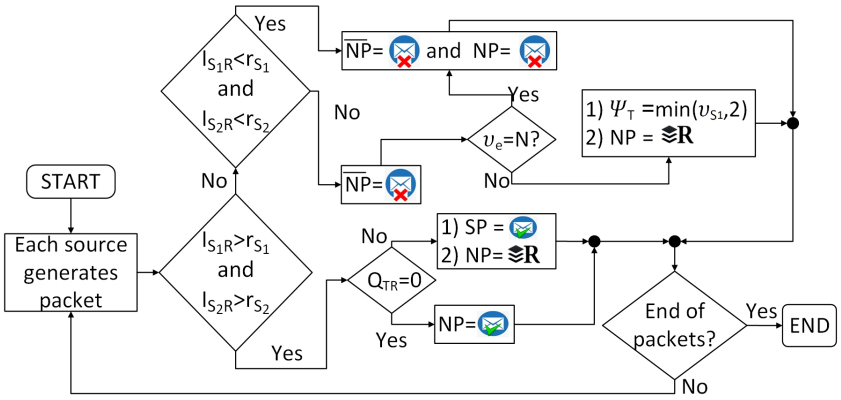


Figure 6. Scenario 3: With only Single-Buffer in the relay node.

- As in Scenario 2, if both links are not available, the new packets from nodes S_1 and S_2 are lost.
- If all links are available, the relay first transmits the coded packet if it has packets from both directions; otherwise, it receives the packets from each transmitter and then transmits them.
- If one of the links is available and the other is not available, then:
  - On the available link: First, the packet ready to be sent on the relay is transmitted to its destination; then, the sender sends the generated packet to the relay if its buffer is not full; otherwise, the packet is lost.
  - On the unavailable link, the associated packet is lost.

An example of the three possibilities is when all links are available and $Q_{TR} = 0$; then, S_1 transmits to R, S_2 transmits to R, and R broadcasts. The reference signal sent by the relay contains the information of this transmission order. As in Scenario 2, the proposed Algorithm 2 can increase the number of transmitted packets only when one of the symmetric channels is available. For example, using Algorithm 2 when the link $S_1 \rightleftharpoons R$ is available, and the link $S_2 \rightleftharpoons R$ is unavailable, and the number of elements in the single buffer destined to S_1 is greater than or equal to 2, the relay sends two packets and receives one.

Algorithm 2 Scenario 3 transmission algorithm

Input Q_T, Q_R, L, I_{S_1R}, I_{S_2R}, R_{S_1}, R_{S_2}.
Require: $(I_{S_1R} >= R_{S_1}$ and $I_{S_2R} < R_{S_2})$ or $(I_{S_1R} < R_{S_1}$ and $I_{S_2R} >= R_{S_2})$
1: $n_1 \leftarrow 2$
2: $y \leftarrow 1, 2$
3: **if** $v_{S_y} >= 2$ **then**
4: $\psi_T \leftarrow 2$
5: $\psi_R \leftarrow 1$
6: **end if**
Output ψ_T, ψ_R

3.4. Scenario 4: Two Separate Buffers on the Relay and One Buffer on Each Transmitter Node

The use of buffers in the transmitters would allow that, in the worst conditions of the channel, the transmitters could temporarily store the information while waiting for the channel to improve in the next time slots. Although, for example, it is admitted that the two links of the system model are not available in a time slot, in this case, the use of a buffer at the transmitter would allow for temporarily storing the information generated in the source

buffer. Another case of using buffers in transmitters could be in a network composed of multiple relays, where the statistical analysis could be simplified only when one relay acts as a transmitter, another as a relay, and the last as a destination. Thus, forming a system of transmitter, relay, and destination using a buffer in all nodes.

In this subsection, the procedures used to model Scenario 4 are shown. Let K_S and $\overline{K_S}$ denote the source buffer state associated with the available link and the source buffer state associated with the unavailable link, respectively. In other words, in this scenario, if the link $S_1 \rightleftharpoons R$ is available and the link $S_2 \rightleftharpoons R$ is unavailable, then the state of B_{S_1} is K_S, and the state of B_{S_2} is $\overline{K_S}$. Figure 7 shows the flowchart of all the possibilities that exist in Scenario 4. Based on CSI/BSI, the relay sends a reference signal enabling the following events:

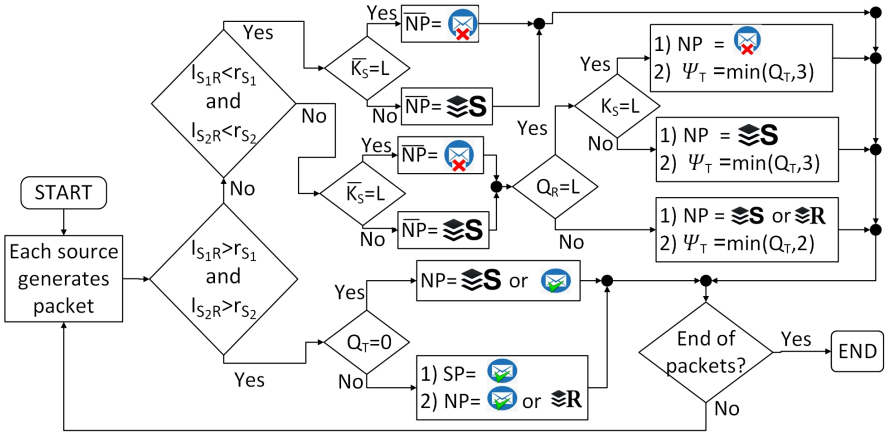


Figure 7. Scenario 4: With a Buffer in all nodes.

- If both links are not available, the generated packets are stored in the source buffer (S_1 or S_2) or are lost according to the state of the source buffer.
- If both links are available, the packet generated by S_1 is sent to the destination, or is sent to the relay to be stored, or is stored in S_1 according to the capabilities of the buffers of S_1 and of R. The same happens with the packets that are generated in the node S_2.
- If one of the links is unavailable and the other is available, then:
  - The generated packet associated with the unavailable link is stored in the source buffer or is lost depending on the state of the source buffer.
  - The packet generated on the available link is stored in the corresponding source buffer, sent to the relay node, or lost. Packets in the buffer of the relay are sent according to sub-time-slot availability.

Algorithm 3 shows the mechanism used to increase the number of transmissions per time slot when only one of the links is unavailable. This algorithm can transmit up to three packets when only one channel is available, which does not happen when the algorithm is not used. According to Algorithm 3, when the receiver buffer is not full, if the source buffer associated with the available link is empty, the relay can send up to two packets and receive the new packet generated at the source. When the receiver buffer is full, the relay can only transmit up to three packets, depending on the number of packets stored in the sender buffer. This is because, in this time slot when the receiver buffer is full, the relay decides not to receive the packet due to a lack of buffer space. These examples make it possible to increase the number of packets transmitted per time slot.

Algorithm 3 Scenario 4 transmission algorithm

Input Q_T, Q_R, L, I_{S_1R}, I_{S_2R}, R_{S_1}, R_{S_2}, v_{S_1} ,v_{S_2}.
Require: $(I_{S_1R} >= R_{S_1}$ and $I_{S_2R} < R_{S_2})$ or $(I_{S_1R} < R_{S_1}$ and $I_{S_2R} >= R_{S_2})$
$n_{1,2,3} \leftarrow 1, 2, 3$
$y \leftarrow 1, 2$
if $Q_R = L$ **then**
    $\psi_T \leftarrow \min(3, Q_T)$
else
    if $v_{S_y} = 0$ **then**
        $\psi_T \leftarrow \min(n_2, Q_T)$; $\psi_R \leftarrow n_1$
    else if $v_{S_y} = 1$ **then**
        if $Q_R = L - 1$ **then**
            $\psi_T \leftarrow \min(n_2, Q_T)$; $\psi_R \leftarrow n_1$
        else
            $\psi_T \leftarrow n_1$; $\psi_R \leftarrow n_2$
        end if
    else if $v_{S_y} = 2$ **then**
        if $Q_R = L - 1$ **then**
            $\psi_T \leftarrow \min(n_2, Q_T)$; $\psi_R \leftarrow n_1$
        else if $Q_R = L - 2$ **then**
            $\psi_T \leftarrow n_1$; $\psi_R \leftarrow n_2$
        else
            if $Q_T = L$ **then**
                $\psi_T \leftarrow n_1$; $\psi_R \leftarrow n_2$
            else
                $\psi_T \leftarrow n_2$; $\psi_R \leftarrow n_1$
            end if
        end if
    else if $v_{S_y} \geq 3$ **then**
        if $Q_R = L - 1$ **then**
            $\psi_T \leftarrow \min(n_2, Q_T)$; $\psi_R \leftarrow n_1$
        else if $Q_R = L - 2$ **then**
            $\psi_T \leftarrow n_1$; $\psi_R \leftarrow n_2$
        else
            if $Q_T = 0$ **then**
                $\psi_R \leftarrow n_3$
            else
                $\psi_T \leftarrow n_1$; $\psi_R \leftarrow n_2$
            end if
        end if
    end if
end if
Output ψ_T, ψ_R

3.5. Scenario 5: Single Buffer on the Relay and a Buffer on Each Transmitter Node

This scenario combines Scenarios 3 and 4, taking advantage of a set of benefits obtained in terms of OP. It implements a single buffer on the relay and buffers on the transmitters. With the implementation of the single buffer, it is expected to improve even more the results of Scenarios 3 and 4. Figure 8 presents the different possibilities (cases) of this scenario. In each time slot, the relay sends a reference signal based on BSI/CSI. This signal enables the following three events to occur.

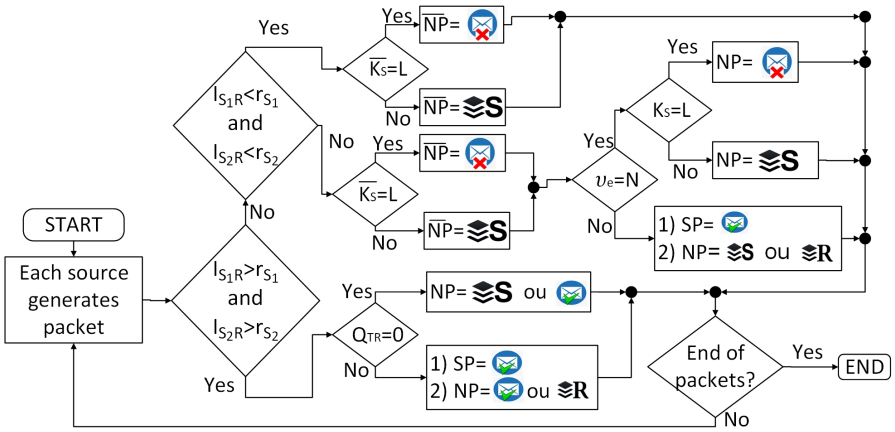


Figure 8. Scenario 5: With a single buffer in the relay node and a buffer in the transmitter node.

- As in Scenario 4, if both links are not available, the generated packet is stored (at the transmitter) or is lost according to the state of the buffer source.
- If all links are available, the new packet of S_1 is sent to its destination, or is sent to the relay to be stored, or is stored in S_1 according to the capacity of S_1 and sub-slot time availability. The same happens with the packets that are generated in the node S_2. The organization of packets from both directions takes place in a single buffer.
- If one of the links is available and the other is not then:
  - On the available link: The packet on the relay ready to be sent is transmitted to its destination according to Algorithm 4, and the newly generated packet is either stored in the retransmission buffer or is stored in the source buffer or is lost.
  - In the unavailable link, the packet generated by the transmitter is lost or stored in the source buffer.

Algorithm 4 Spectral efficiency algorithm in Scenario 5

Input Q_T, Q_R, L, I_{S_1R}, I_{S_2R}, R_{S_1}, R_{S_2}, N, v_{S_1} ,v_{S_2}.
Require: for $(I_{S_1R} < R_{S_1}$ and $I_{S_2R} \geq R_{S_2})$ $X_1 \leftarrow v_{S_1}$
Require: for $(I_{S_1R} \geq R_{S_1}$ and $I_{S_2R} < R_{S_2})$ $X_1 \leftarrow v_{S_2}$
$n_{1,2,3} \leftarrow 1, 2, 3$
$y \leftarrow 1, 2$
if $X_1 = 0$ **then**
  if $Q_{TR} = N - 2$ **then**
    $\psi_R \leftarrow \min(n_2, v_{S_y})$
  else if $Q_{TR} <= N - 3$ **then**
    $\psi_R \leftarrow \min(n_3, v_{S_y})$
  end if
else if $X_1 = 1$ **then**
  if $Q_{TR} < N$ **then**
    $\psi_T \leftarrow n_1$; $\psi_R \leftarrow \min(2, v_{S_y})$
  end if
else
  $\psi_T \leftarrow n_2$; $\psi_R \leftarrow n_1$
end if
Output ψ_T, ψ_R

As in Scenario 4, when the two links are unavailable, this scenario also makes it possible to store the packet in the source buffer, as long as it is not full. Algorithm 4 shows the mechanism used to increment the number of transmissions per time slot. For example, if the link $S_1 \rightleftharpoons R$ is available, the link $S_2 \rightleftharpoons R$ is unavailable, and $v_{S_1} > 1$, then the relay sends two packet units and receives one from the transmitter S_1. This

strategy allows for releasing a unit single buffer, ensuring buffer availability for the next time slots. Furthermore, it allowed for incrementing of up to three of the total number of sent/received packets using Algorithm 4. In general, using the proposed algorithm can allow the freeing space in the buffers, guaranteeing the availability of buffers in the next time slots. Furthermore, they can reduce the delay of packets in the system by taking advantage of the three available sub-time slots. In the next section, the analytical models of the scenarios are developed.

4. Analysis and Implementation

4.1. Analysis without Buffer Implementation

In this section, the individual outage probability and the system outage probability of Scenario 1 are determined. According to [29,57], the probability that S_1 fails to communicate with S_2 is given by:

$$\mathcal{O}_{S_1} = \mathcal{P}(\min\{I_{S_1R}, I_{RS_2}\} < r_i). \tag{4}$$

Substituting (2) into (4), we obtain:

$$\begin{aligned}
\mathcal{O}_{S_1} &= \mathcal{P}\left\{\min\left[\frac{1}{3}\log\left(1+\frac{|h_{S_1R}|^2 P_{S_1}}{P_n}\right), \frac{1}{3}\log\left(1+\frac{|h_{RS_2}|^2 P_R}{P_n}\right)\right] < r_{S_1}\right\} \\
&= \mathcal{P}\left[\log\left(1+\frac{|h_{S_1R}|^2 P_{S_1}}{P_n}\right) < 3r_{S_1}\right] + \mathcal{P}\left[\log\left(1+\frac{|h_{S_1R}|^2 P_{S_1}}{P_n}\right) \geq 3r_{S_1}\right]\mathcal{P}\left[\log\left(1+\frac{|h_{RS_2}|^2 P_R}{P_n}\right) < 3r_{S_1}\right] \\
&= \mathcal{P}\left[\frac{|h_{S_1R}|^2 P_{S_1}}{P_n} < 2^{3r_{S_1}}-1\right] + \mathcal{P}\left[\frac{|h_{S_1R}|^2 P_{S_1}}{P_n} \geq 2^{3r_{S_1}}-1\right]\mathcal{P}\left[\frac{|h_{RS_2}|^2 P_R}{P_n} < 2^{3r_{S_1}}-1\right] \\
&= \mathcal{P}\left[|h_{S_1R}|^2 < \frac{a_{S_1}-1}{\rho_{S_1}}\right] + \mathcal{P}\left[|h_{S_1R}|^2 \geq \frac{a_{S_1}-1}{\rho_{S_1}}\right]\mathcal{P}\left[|h_{RS_2}|^2 < \frac{a_{S_1}-1}{\rho_R}\right] \\
&= \int_0^{\varepsilon_1 x} \frac{e^{\frac{-x}{\lambda_{S_1R}}}}{\lambda_{S_1R}}dx + \left(1-\int_0^{\varepsilon_1 x}\frac{e^{\frac{-x}{\lambda_{S_1R}}}}{\lambda_{S_1R}}dx\right)\left(\int_0^{\varepsilon_2 x}\frac{e^{\frac{-x}{\lambda_{RS_2}}}}{\lambda_{RS_1}}dx\right) \\
&= \left(1-e^{-\frac{1}{\lambda_{S_1R}}\frac{a_{S_1}-1}{\rho_{S_1}}}\right) + \left(e^{-\frac{1}{\lambda_{S_1R}}\frac{a_{S_1}-1}{\rho_i}}\left(1-e^{-\frac{1}{\lambda_{RS_2}}\frac{a_{S_1}-1}{\rho_R}}\right)\right),
\end{aligned} \tag{5}$$

where $\varepsilon_1 = \frac{a_{S_1}-1}{\rho_{S_1}}$, $\varepsilon_2 = \frac{a_{S_1}-1}{\rho_R}$, $\rho_R = P_R/P_n$, $\rho_{S_1} = P_{S_1}/P_n$, $a_i = 2^{3r_i}$ and $r_i, i \in \{1,2\}$ is the target rate for the nodes S_1 and S_2, respectively. For $\mathcal{O}_{S_2}$, it is enough to change S_1 into S_2 and S_2 into S_1 in (5).

In this way, the pair outage probability is given by:

$$\mathcal{O}_{Pair} = \mathcal{O}_{S_1} \cup \mathcal{O}_{S_2}. \tag{6}$$

4.2. Markov Model for Scenarios with Buffer

In this subsection, the proposed solutions to model scenarios that implement buffers are described through Markov chains (MC).

4.2.1. Markov Model for Scenario 2

In Figure 9, Scenario 2 is modeled using an MC where the possible transition states of the buffer are represented. Buffer transition states are the occupancy of the buffer on each transmission. This model describes the behavior of the packets in the buffer of the relay queue in terms of increase, decrease, or remaining in the same state depending on the availability or not of the link and the buffer space. The buffer transition states are denoted

A_1 and A_2 where A_1 is the state of buffer B_{S_1R} and A_2 is the state of buffer B_{S_2R}. However, A_3 and A_4 represent the link state of S_1R and S_2R, respectively (Figure 9).

The modeling expresses the individual outage probability of S_1. Furthermore, the transition state diagram is designed for a maximum buffer size of three to guarantee the exploitation of the three available time sub-time-slots. Given the system complexity, to derive the expression that calculates the OP of S_1, all the events that lead to a link outage are modeled using the information from the state diagram obtained from Figure 9. As in this figure, in Table 3, the buffer and link states are represented similarly. We denote "YES" when an outage event occurs and "NO" when an outage event does not occur.

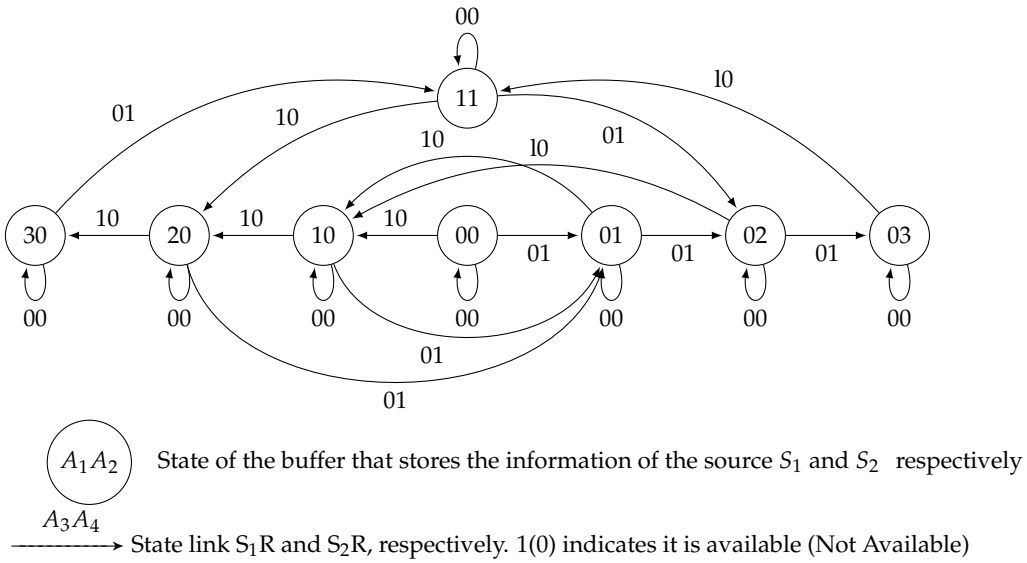


Figure 9. State transition diagram of Scenario 2.

Table 3. Outage events.

Buffer State \ Link State	00	01	10
00	Yes	Yes	No
10	Yes	Yes	No
01	Yes	Yes	No
11	Yes	Yes	No
20	Yes	Yes	No
02	Yes	Yes	No
30	Yes	Yes	Yes
03	Yes	Yes	No

It could be noticed that Table 3 describes all the possible events that lead to an outage considering the buffer current state and the condition of each link. For example, when the buffers are empty and the two links are not available, then an outage event ("Yes") occurs according to Table 3. In general, eight possible events leading to outage due to link unavailability and one event leading to outage due to buffer space unavailability are observed. Taking into account the eight possible state transitions of the MC, the OP from S_1 to S_2 is given by:

$$\begin{aligned}\mathcal{O}_{S_1} &= \frac{1}{8}\left[8\mathcal{O}_{S_1R} + \left(1-\mathcal{O}_{S_1R}\right)\left(\mathcal{O}_{RS_2}\right)\right] \\ &= \left(1 - e^{-\frac{1}{\lambda_{S_1R}}\frac{a_{S_1}-1}{\rho_{S_1}}}\right) + \frac{1}{8}e^{-\frac{1}{\lambda_{S_1R}}\frac{a_{S_1}-1}{\rho_{S_1}}}\left(1 - e^{-\frac{1}{\lambda_{RS_2}}\frac{a_R-1}{\rho_R}}\right).\end{aligned} \tag{7}$$

The transition matrix for Scenario 2, considering the state diagram, can be written as follows:

$$\boldsymbol{M} = \begin{bmatrix} \overline{P_1P_2} & \overline{P_1}P_2 & P_1\overline{P_2} & 0 & 0 & 0 & 0 & 0 \\ 0 & \overline{P_1P_2} & P_1\overline{P_2} & \overline{P_1}P_2 & 0 & 0 & 0 & 0 \\ 0 & \overline{P_1}P_2 & \overline{P_1P_2} & 0 & P_1\overline{P_2} & 0 & 0 & 0 \\ 0 & 0 & P_1\overline{P_2} & \overline{P_1P_2} & 0 & \overline{P_1}P_2 & 0 & 0 \\ 0 & \overline{P_1}P_2 & 0 & 0 & \overline{P_1P_2} & 0 & P_1\overline{P_2} & 0 \\ 0 & 0 & 0 & 0 & 0 & \overline{P_1P_2}+\overline{P_1}P_2 & 0 & P_1\overline{P_2} \\ 0 & 0 & 0 & 0 & 0 & 0 & \overline{P_1P_2}+P_1\overline{P_2} & \overline{P_1}P_2 \\ 0 & 0 & 0 & \overline{P_1}P_2 & P_1\overline{P_2} & 0 & 0 & \overline{P_1P_2}, \end{bmatrix} \tag{8}$$

where $\overline{P}_1$ and $\overline{P}_2$ are the outage probability of links $S_1 \rightleftharpoons R$ and $S_2 \rightleftharpoons R$, respectively. $\overline{P}_1$ and $\overline{P}_2$ can be expressed through Equation (3), $P_1 = 1 - \overline{P}_1$ and $P_2 = 1 - \overline{P}_2$. A steady-state probability can be expressed as:

$$\boldsymbol{\pi} = (\mathbf{M} - \mathbf{I} + \mathbf{B})^{-1}\mathbf{b}, \tag{9}$$

where $\mathbf{I}$ is the identity matrix, $\mathbf{B}$ is a 8×8 matrix with all elements equal to one, $\mathbf{b} = [1, \ldots, 1]^T_{1\times 8}$ and $\boldsymbol{\pi} = [\pi_1, \ldots, \pi_8]$.

4.2.2. Markov Model for Scenario 3

Figure 10 illustrates the seven levels of the possible states of Scenario 3, where the evolution of the possible states of the MC is described. It is important to note that having a single buffer implies that the storage capacity is twice than that of Scenario 2. Each state in the transition diagram describes the current state of the buffer and the total number of packets from each destination stored in the buffer. In other words, A_5 presents the state of the buffer, while A_6 and A_7 represent the number of items in the destination S_1 and S_2, respectively. An illustrative example is state 312, where there are three buffered packets, one from destination S_2 and two from destination S_1.

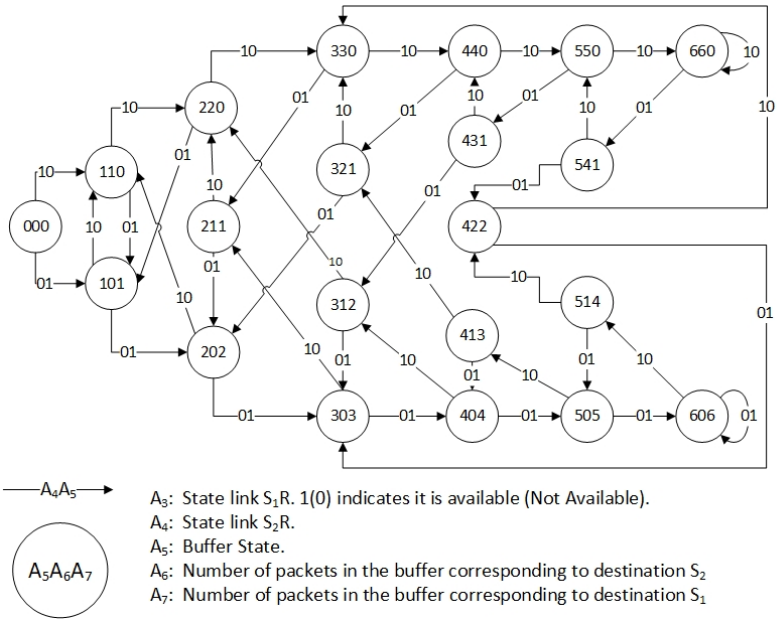


Figure 10. State transition diagram of Scenario 3.

Transitions from one state to another occur when there is space in the buffer, and only one link is available. The state remains the same when, in seven consecutive attempts, the samples have exactly the same channel condition. Consequently, for a buffer capacity of six, we have seven possible states. As in Scenario 2, the expression for OP is derived similarly, except for the outage event caused by the unavailability of the relay storage space. This outage event only occurs if one link is available and the other is unavailable for seven or more simultaneous time slots. Thus, the expression for the outage probability is given by:

$$\begin{aligned}\mathcal{O}_{S_1} &= \frac{1}{7}\left[7\mathcal{O}_{S_1R} + \left(\mathcal{O}_{RS_2}\left(1-\mathcal{O}_{S_1R}\right)\right)^7\right] \\ &= \left(1-e^{-\frac{1}{\lambda_{S_1R}}\frac{a_{S_1}-1}{\rho_{S_1}}}\right) + \left[\frac{1}{7}e^{-\frac{1}{\lambda_{S_1R}}\frac{a_{S_1}-1}{\rho_{S_1}}}\left(1-e^{-\frac{1}{\lambda_{RS_2}}\frac{a_R-1}{\rho_R}}\right)\right]^7.\end{aligned} \tag{10}$$

In Scenario 3, we limit ourselves to presenting the state diagram and the outage probability since the state transition matrix becomes denser and provides little information for the obtained results. Besides the state of the buffer, to represent the matrix, two additional states to represent the packet numbers of each transmitter are also required. In addition, in Scenarios 4 and 5, we limited ourselves only to the numerical models developed in Sections 3.4 and 3.5 due to the complexity of the Markov Chain of four or three buffers with a minimum size of three for each one.

4.3. Practical Considerations

This section presents some practical considerations for implementing the model. First, it is necessary to formulate a buffer size optimization problem based on the trade-off that it represents in terms of cost-effectiveness. That is, as the buffer size increases, the outage probability decreases, but the hardware cost increases. Therefore, finding the optimal buffer size value that gives the desired result is essential. Furthermore, if the channel between the source and the relay was asymmetrical, a power control-based approach would be required, since the transmission channel may be available while the receiving channel may not. The same can be achieved by limiting the SNR to a minimum required value and limiting the maximum transmit power. However, in this article, when considering a symmetrical channel, both the transmitter and the receiver perceive the same CSI. In other words, there is no need to pose a problem based on power control, as the information sent can be successfully received. Another critical problem for implementing our proposal could be the Jamming Attack in an asymmetric channel situation. This can occur when the receiver experiences severe fading or is exposed to interference. In this situation, the receiver cannot receive information but can take this opportunity to transmit the packet(s) stored in the buffer.

Furthermore, it is worth noting that our model considers that there is no direct link between the two sources, S_1 and S_2. This scenario is common in urban areas with many buildings, where the fading of the infrastructure between the two sources is very high. In the most critical scenarios, drone-assisted communication solutions have even been proposed, which can reach advantageous positions to act as relays [58]. However, this system model could be generalized considering a direct link between the two sources. Depending on the zone type, this approach could increase the system's reliability. Different from the existing proposals, ours proposes a minimum buffer size equal to three to explore the three-time slots to reduce the system outage probability.

Additionally, in simple buffer scenarios, there is a need to reserve memory space to save information on the transmission direction of each packet and thus guarantee the send order and the correct destination. Note that this mapping can be completed by relating the value (0 or 1) of a bit to each buffer position.

5. Simulation and Numerical Results

In this section, numerical results are presented to evaluate the performance of the five scenarios in terms of OP. Table 4 shows the parameters used in this paper unless otherwise specified.

Table 4. System parameters.

Parameter	Symbol	Value
Packet sample number	Sample	10^6
Relay position	d_{S_1R}	0.500
Path loss exponent	α	4
Noise power	P_n	1
Minimum separate buffer size	L	3
Minimum size of single buffer	N	6
Target transmission rate	r_i	1 bpcu
Transmission power	P	10 dB
Signal-to-noise ratio measured at the transmitter side	ρ	10 dB

Initially, all buffers are empty and distances are normalized with reference to $d_{S_1S_2}$. To simplify the analysis, it is assumed that the transmission powers of the three nodes are equal and denoted by P, that is, $P_{S_1} = P_{S_2} = P_R = P$ and, consequently, $\rho_{S_1} = \rho_{S_2} = \rho_R = \rho$. The power is normalized with respect to the noise power, and we consider a unit bandwidth throughout the article. Simulations are performed in MATLAB software with a million Monte Carlo events. Unless otherwise stated, we consider three for the minimum value of the separated buffer, six for the minimum value of the single buffer, and limiting the maximum buffer size of the separated buffer to six and the single buffer to twelve. The results of article [59] inspired some of the parameter values used. In [60], we uploaded on GitHub the functions written in MATLAB to reproduce the results.

Figure 11 shows the packet loss rate with different sample numbers of packets in the scenarios using buffers for different values of SNRs. It is observed from Figure 11a that, for 7×10^5 analyzed packets with SNR equal to -10 dB, approximately 95% are lost for the four evaluated scenarios. The same is true for 9×10^5 sample packets, where approximately 94% of the parsed packets are lost.

On the other hand, in Figure 11c, for 7×10^5 analyzed packets with SNR equal to 10 dB, approximately 5% are lost in Scenario 2, 4.160% in Scenarios 3 and 4, and 2.280% in Scenario 5. Thus, it can be partially concluded that, with SNR equal to -10 dB, the scenarios with buffer usage lose approximately the same amount of packets, and almost all analyzed packets are lost. However, with SNR equal to 10 dB, not only does the packet loss rate decrease, but the buffering strategy in all nodes (Scenario 5) provides a low packet loss rate compared to the other scenarios.

Additionally, in Figure 11d, for a sample of 9×10^5 packets, the red and green bars of the buffer usage scenarios on the relay only show that approximately 0.500% and 0.440% of the packets are lost, respectively. However, Scenarios 4 and 5 show approximately 0.420% and 0.280% of packets lost, respectively. The same behavior can be observed in Figure 11c. It can be partially concluded that the strategy of using a single buffer in the relay allows for obtaining a lower packet loss rate compared to the use of two separate buffers in the relay. Furthermore, the proposal of buffering at the transmitters and a single buffer at the relay shows less packet loss than the proposal of buffering at the transmitters and a separate buffer at the relay. This further proves the benefits that the use of a single buffer can bring.

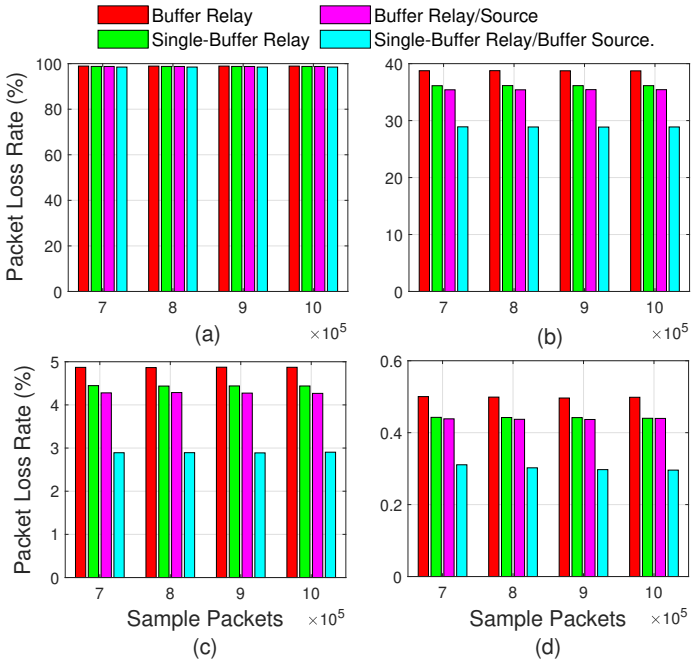


Figure 11. Packet loss rate for different values of SNR: (**a**) $\rho = -10$ dB; (**b**) $\rho = 0$ dB; (**c**) $\rho = 10$ dB; (**d**) $\rho = 20$ dB.

In summary, the use of a single buffer shows that fewer packets are lost compared to the strategy of using separate buffers in the relay. In addition, the proposal of the buffer in the transmitters and a single buffer in the relay showed better results in terms of packet loss rate.

5.1. Individual Outage Probability

Figure 12 shows the result of the Monte Carlo simulation together with the analytical results obtained from (5), (7), (10) of the unbuffered models, with buffers separated in the relay, and with the single buffer on the relay, respectively. First, it is observed that numerical simulations coincide with analytical simulations, which validates the system model. It can also be seen that the use of single and separate buffers in the relay brings a significant benefit to the system model as it gives us less OP compared to the unbuffered model. For example, for SNR equal to 0 dB, the blue curve of Scenario 1 [29] shows an OP of 0.583 while the red and green curves of Scenarios 2 [39,47] and 3 show an OP of 0.389 and 0.345, respectively. Likewise, with SNR equal to 10 dB, an OP of 0.083, 0.047, and 0.042 is obtained in Scenarios 1, 2, and 3 of the blue, red, and green curves, respectively—thus representing a difference of 0.040 between buffered and unbuffered scenarios.

Furthermore, when an outage probability of 0.100 is required in the system, the unbuffered scheme achieves it with an SNR of 8.500 dB, while the two buffer usage schemes in the relay achieve it with an SNR of approximately 6.500 dB.

Other results to be highlighted are the OP values obtained in Scenarios 2 and 3. For example, for SNR equal to 5 dB, Scenario 2 shows an OP of 0.143 while Scenario 3 shows an OP of 0.129, a difference of approximately 11.080%. Although this difference between OP in Scenarios 2 and 3 is not significant, for delay non-tolerant packets, using a single buffer (the green curve results) can be more efficient compared to using a separate buffer in the relay. Furthermore, using a single buffer allows for the efficient use of hardware. This is because, in Scenario 3, fewer transition states are needed than in Scenario 2.

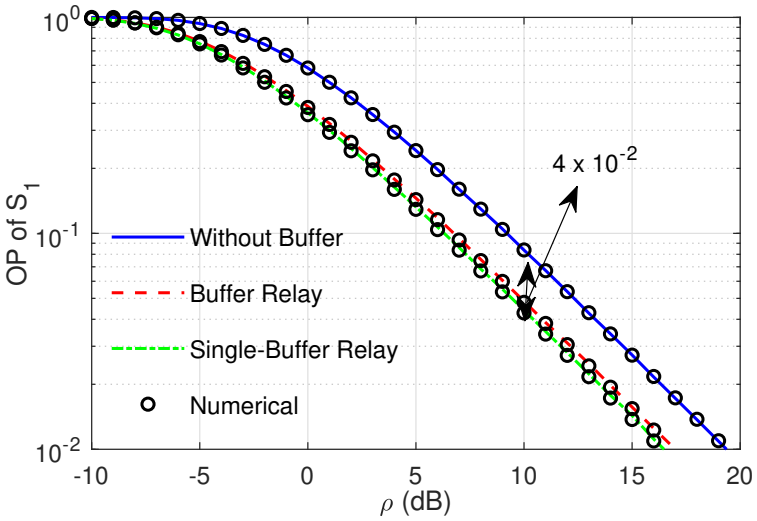


Figure 12. Channel outage probability from S_1 to S_2 as a function of SNR for Scenario 1 [29], Scenario 2 [39,47], and Scenario 3.

Figure 13 shows the OP as a function of the SNR. A greater benefit in terms of OP is achieved when implementing buffering in all transmitting nodes. For example, when SNR equals 0 dB, the curve for Scenario 4 reaches an OP of 0.315, while the curve for Scenario 5 reaches an OP of 0.294. Similar results are obtained for SNR equal to 10 dB, where OPs of 0.036 and 0.029 are achieved for Scenarios 4 and 5, respectively.

It can be partially concluded that the single-buffer scenario in the relay, together with a buffer in the transmitter, provides better benefits mainly in OP than the other scenarios discussed.

Furthermore, when an OP of 0.020 is required in the system, Scenario 4 achieves it with SNR equal to 11.500 dB while Scenario 5 achieves it with 12,500 dB, thus representing a gain of 1 dB. Furthermore, with the same system requirements, Scenarios 2 and 3 achieved them with SNR equal to 14 dB, while Scenario 1 needs 16,500 dB. It turns out that our proposal requires less SNR compared to existing ones to meet a predetermined outage probability requirement.

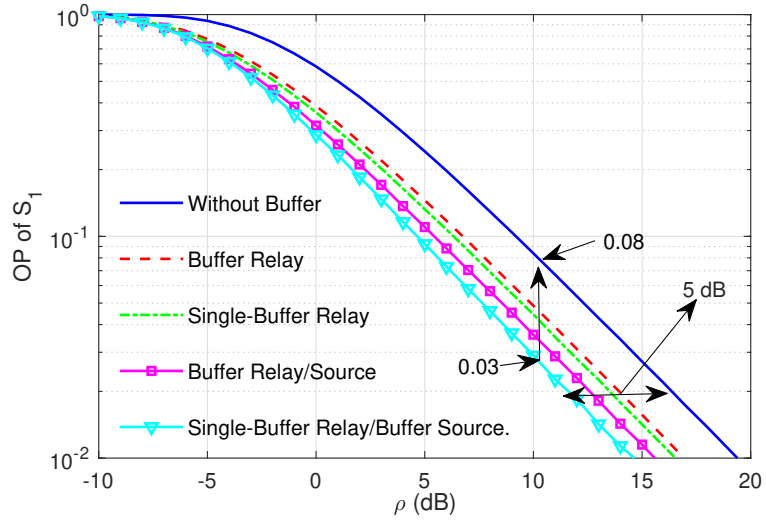


Figure 13. Channel outage probability from S_1 to S_2 as a function of SNR with $r_i = 1$ bpcu.

Figure 14 shows the OP as a function of the target transmission rate in the five investigated scenarios. It can be seen that the target transmission rate has an impact on the OP of the system in all the discussed scenarios.

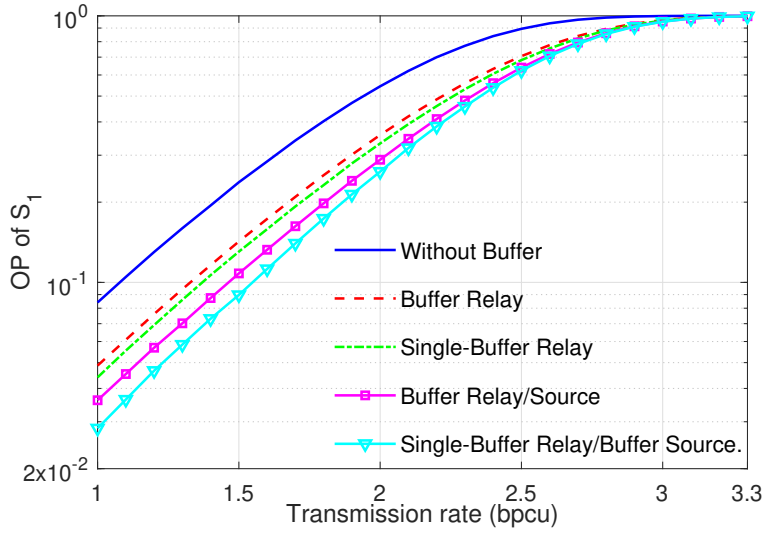


Figure 14. Channel outage probability from S_1 to S_2 as a function of target transmission rate with SNR equal to 10 dB.

For example, with SNR equal to 10 dB, an OP of 0.100 is achieved with a rate of 1.100 bpcu in Scenario 1, 1.300 bpcu in Scenario 2, 1.350 bpcu in Scenario 3, 1.400 bpcu in Scenario 4, and finally 1.600 bpcu in Scenario 5. Furthermore, with the same SNR and with a target transmission rate equal to 1.500 bpcu, the blue curve in Scenario 1 reaches an OP of 0.237. In comparison, for a target transmission rate equal to 2 bpcu, the same curve reaches an OP of 0.544, thus representing an increment of 122.900%. Furthermore, with SNR equal to 10 dB and a target transmission rate equal to 2 bpcu, Scenario 5 reaches an OP of 0.260, while for a target transmission rate equal to 2.500 bpcu, the OP increments up to 0.622. Scenarios 2, 3, and 4 also show an increase in OP whenever target transmission rates increase. When the system model requires a lower OP, our schemes achieve it with a lower target transmission rate. Furthermore, for a target transmission rate equal to 3 bpcu, the five investigated scenarios show the worst results.

Figure 15 shows the individual OP of the transmitters S_1 and S_2 of the five analyzed scenarios when the distance d_{S_1R} is varied with different sizes of the buffer. In each of the investigated scenarios, the ideal distance that improves the individual OP to the transmitters S_1 and S_2 is obtained. For example, in Figure 15a, the optimal distances that improve the performance of the individual OP of the transmitter S_1 of Scenarios 4 and 5 are approximately equal to 0.510 and 0.416, respectively.

In Figure 15b, the optimal distances of the individual OP of the transmitter S_2 of Scenarios 4 and 5 are approximately equal to 0.490 and 0.584, respectively. Another expected result is the reflected symmetry of the curves in Figure 15a,b. This symmetry is due to the identical conditions and configurations of the two transmitter nodes since the relay can only be at a fixed point between the two transmitters.

Additionally, it can also be observed that, for all investigated scenarios, the individual OP converges to the same performance when the relay node is farthest from the transmitting node or when it is positioned at a greater than optimal distance. For example, in Figure 15a,c, for a distance equal to 0.800, the individual OP of S_1 of the five investigated scenarios gives the same result. The same happens in Figure 15b,d with a distance equal to 0.200, in this case for an individual OP of S_2. It can be partially concluded that, for distance equal to 0.200, the models with buffer would be an inadequate option for the system model due to the same results obtained with the model without buffer.

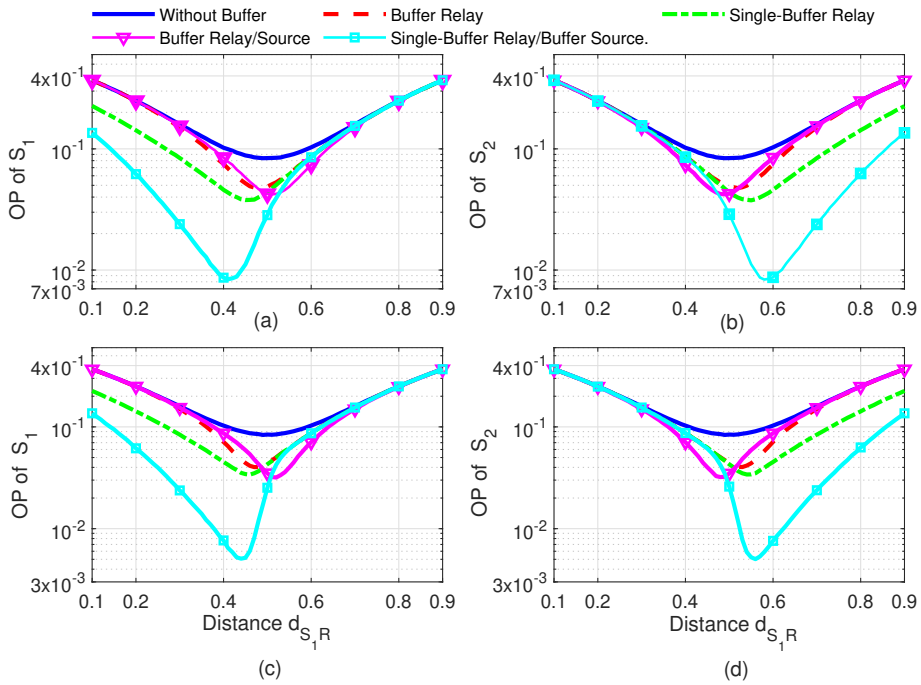


Figure 15. Outage probability of S_1 and S_2 as a function of d_{S_1R} with $r_i = 1$, SNR $= 10$ dB, and buffer in one of the sources (**a**) S_1 with $L = 3$, (**b**) S_2 with $L = 3$, (**c**) S_1 with $L = 6$, and (**d**) S_1 with $L = 6$.

Furthermore, it can be seen that, for a distance interval d_{S_1R} between 0.200 and 0.400, Scenarios 2 and 4 show approximately the same performance in terms of the OP of S_1. However, for Scenarios 3 and 5, we see different performances in terms of OP of S_1. For example, in Figure 15c, for $d_{S_1R} = 0.300$, it is observed that the OP of S_1 of the Scenario 3 is 0.074, while in Scenario 5, the OP of S_1 is 0.023, representing a difference of 0.051. Furthermore, for the same distance, the red and magenta curves of Scenarios 2 and 4 show approximately an OP of S_1 equal to 0.154 in the same figure. The same findings were made in Figure 15d. Finally, it can be seen that the use of a single buffer on the relay shows better results when the relay is closer to the transmitter. Furthermore, the greater the capacity of buffers of the system, the better the result obtained in terms of individual OP.

Figure 16 shows the result of OP when using the optimal distance from Scenario 5. It is observed that, using the optimal distance, a better result is obtained in terms of OP. For example, using this optimal distance with SNR equal to 10 dB, we obtain an OP equal to 0.008. This represents an improvement in terms of OP of approximately four times compared with the results shown in Figure 13 by placing the relay halfway between the two transmitters. This good result is barely noticeable at SNR below 0 dB. Although the ideal distance for Scenario 5 is approximately equal to 0.416, it does not mean that it is the ideal distance for the rest of the scenarios. For example, at this optimal distance from Scenario 5, Scenario 4 has worse performance in the system compared to the one analyzed in Figure 13. On the other hand, when the system requires an outage probability of 0.004, then Scenario 5 achieves it with 12,500 dB while Scenario 3 achieves it with 20 dB. This represents a gain of approximately 7500 dB.

It can be deduced that, if we configure the relay node with this optimal distance, we can observe a satisfactory result for SNR greater than 0 dB. In addition, at this distance, the scenario to be implemented in the system model must be chosen not to harm the performance of the system.

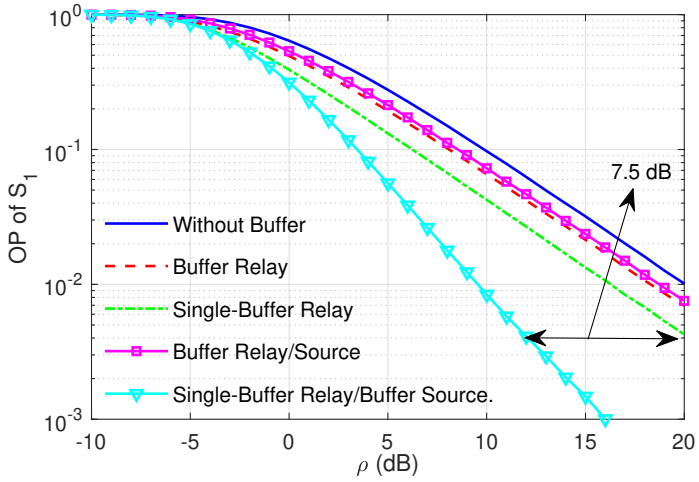


Figure 16. Channel outage probability from S_1 to S_2 as a function of SNR with $r_i = 1$ bpcu and the optimal distance from Scenario 5.

5.2. System Outage Probability

As in Figure 15, in Figure 17, the behavior of the OP of the system is shown by varying the position of the relay with different values of buffer size. Note that, in Figure 17a, when implementing a buffer capacity equal to two, being less than the three available sub-time slots, Scenario 3 shows better results than Scenario 4. For example, for $d_{S_1R} = 0.500$, the magenta curve of Scenario 4 reaches 0.046 of OP of the system while the green curve of Scenario 3 reaches 0.049 of OP of the pair. This is because, for a buffer capacity equal to 2, Scenario 4 does not take full advantage of the three-time slots available at any given time of transmission due to its low storage capacity. In contrast, in Scenario 3, using the single buffer allows for doubling the buffer capacity to 4, providing greater use of the spectrum available in the relay.

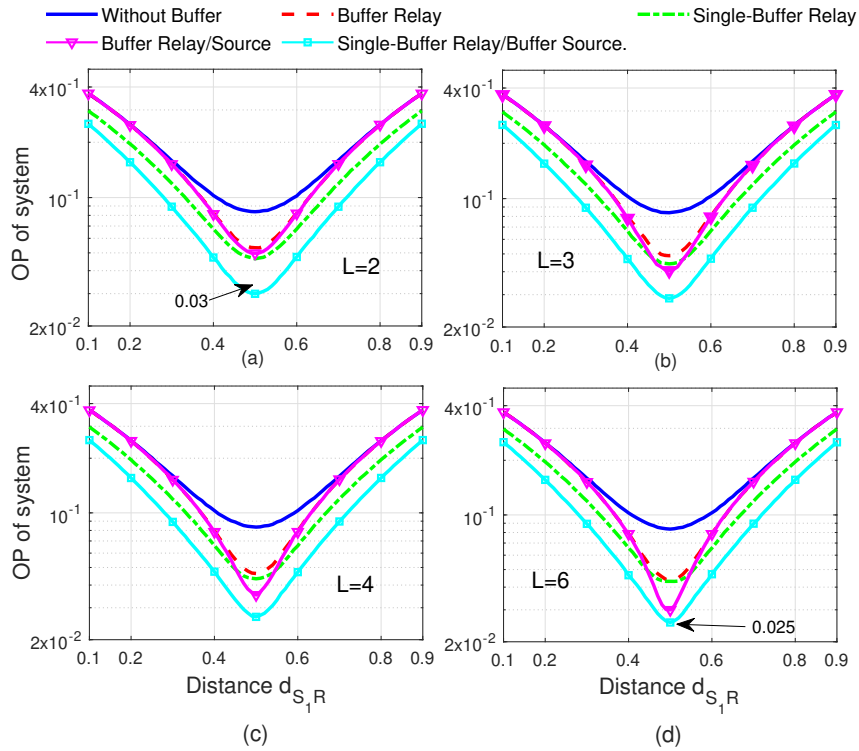


Figure 17. System outage probability as a function of d_{S_1R} for $r_i = 1$ bpcu, $SNR = 10$ dB and different buffer sizes: (**a**) $L = 2$; (**b**) $L = 3$; (**c**) $L = 4$; (**d**) $L = 6$.

The opposite is observed when the minimum buffer size equals the three sub-times slots. Taking the previous example, in Figure 17b, it is observed that the OP of the system of Scenarios 3 and 5 is 0.044 and 0.040, respectively.

Additionally, it can also be observed that the OP of the system of Scenarios 2 and 4 (red and magenta curve) shows a slight variation in the four sub-figures analyzed in Figure 17. However, the opposite happens with the curves of Scenarios 3 and 5; as it is observed that for a larger buffer size, better performance is obtained in terms of OP of the system as shown in Figure 17b,c.

Furthermore, Scenario 3 improves the performance in terms of the OP of the system faster with increasing buffer size than Scenario 5, as seen in Figure 17a,d. This is because the single-buffer concept applies to the buffer of the relay, and as the buffer capacity increases, it directly reflects the size of the single buffer on the relay.

It can be partially concluded that better performance can be obtained if we configure the buffers with a minimum size equal to the three sub-times slots available. Furthermore, to improve performance in terms of system OP, the relay should be positioned between 0.400 and 0.600 but preferably at a distance of 0.500.

Figure 18 shows the energy efficiency of the five scenarios analyzed by varying the position of the relay with different values of buffer size. This metric was calculated as the ratio between the number of packets successfully exchanged between S_1 and S_2 and the number of slots per frame, which in our system model is equal to 3.

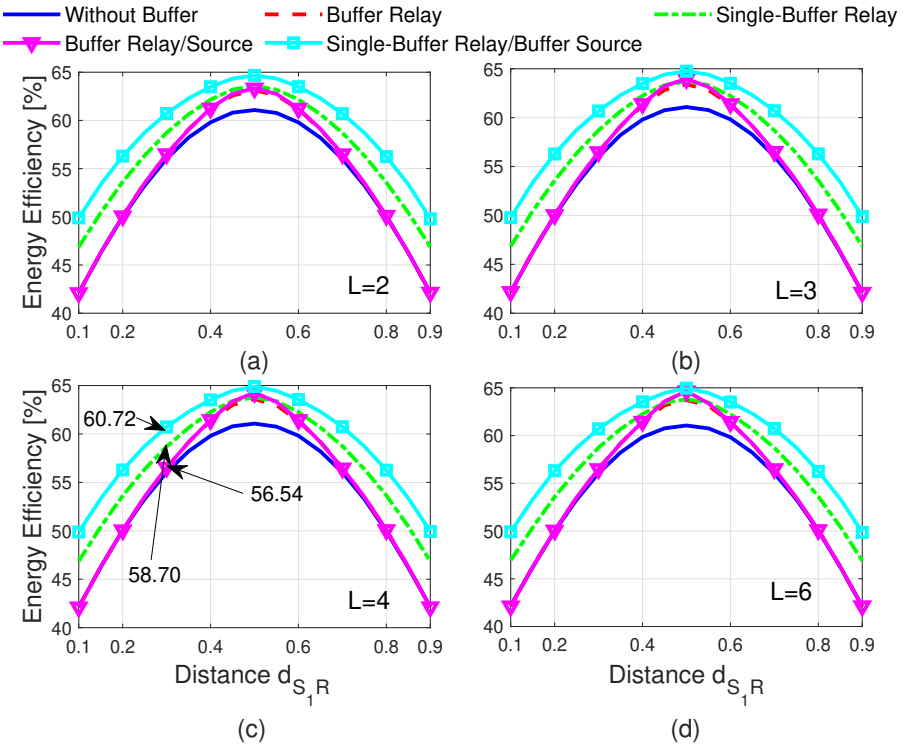


Figure 18. Energy efficiency as a function of d_{S_1R} for $r_i = 1$ bpcu, $SNR = 10$ dB and different buffer sizes: (**a**) $L = 2$; (**b**) $L = 3$; (**c**) $L = 4$; (**d**) $L = 6$.

Note that, for the four sub-figures, Scenarios 2 and 4 (separate buffer scenarios) show approximately the same energy efficiency as the distance from the relay varies. In contrast, Scenarios 3 and 5 (single buffer scenarios) show a gain in energy over the other scenarios, demonstrating that the benefit of increasing the efficiency of the use of the buffer size is of greater impact than that of having a buffer in the transmitters. For example, in Figure 18c, note that, for a distance of 0.3, Scenarios 1, 2, and 4 show approximately an energy efficiency of 56.5%, while Scenarios 3 and 5 show approximately an energy efficiency of 58.7% and

60.7%, respectively. Table 5 summarizes the energy efficiency obtained for the different scenarios analyzed when the relay is at a distance of 0.5 from the source.

Table 5. Energy efficiency of the five scenarios for $d_{S_1R} = 0.5$.

	Energy Efficiency [%] for $d_{S_1R} = 0.5$			
Scenarios	**Figure 18a**	**Figure 18b**	**Figure 18c**	**Figure 18d**
Without Buffer [29]	61.08	61.08	61.08	61.08
Buffer Relay [39,47]	63.12	63.41	63.59	63.73
Single-Buffer Relay	63.58	63.72	63.78	63.82
Buffer Relay/Source	63.36	63.94	64.28	64.65
Single-Buffer Relay /Buffer Source	64.67	64.75	64.89	64.96

Since Scenario 5 outperforms the others in terms of energy efficiency, it can be concluded that the smart scenario selection can significantly improve the system energy efficiency.

6. Conclusions

This paper proposed different buffer usage strategies in a bidirectional network assisted by buffer and channel state information knowledge. The results show that better system performance is obtained when a single buffer of joint use is implemented in the relay and when a buffer is used in the source. Furthermore, it was possible to reduce packet delay and consequently increase the number of received packets through message coding on the relay when the buffer contains messages from both directions. On the other hand, using buffers in all nodes allowed for further improving the performance of the system in terms of outage probability since the transmitter has the capacity to temporarily store the information. We also determine the optimal position of the relay, as well as the required buffer size to provide the best performance in terms of outage probability. In addition, the implementation of a bidirectional network with a single buffer of joint use achieves a notable benefit in terms of energy efficiency for wireless sensor networks. Since unnecessary transmission of information is avoided, the number of idle slots decreases, and the amount of information per unit of time and energy increases.

Although the number of packets received in each time slot was increased through the proposed strategies, the use of buffers in the devices can increase the delay of the packets and cause a loss in the receiver, due to delay constraints and the demanded freshness for the application. For this reason, in future work, we intend to analyze the impact of packet delay to guarantee the quality of service in scenarios that do not tolerate high delays. In addition, it is intended to incorporate energy harvesting, that is, an energy buffer capable of collecting RF energy to take advantage of the inactivity times of the relay and increase the sustainability of the model. On the other hand, we intend to pose a buffer optimization problem to show the cost–benefit relationship of the proposed model. The research showed that bidirectional channels could present various challenges, such as the problem of channel symmetry under interference or jamming attack. For this reason, we intend to address channel symmetry issues, such as jamming attacks or when the channel is considered asymmetric, due to propagation conditions.

Author Contributions: Conceptualization, S.M., S.M.-S.; methodology, S.M., S.M.-S., E.M.G.F., R.D.S.; formal analysis, S.M., S.M.-S.; software, V.F.A., S.M.; validation, S.M., S.M.-S., E.M.G.F., R.D.S.; investigation, V.F.A.; resources, S.M.; writing—original draft preparation, V.F.A.; writing—review and editing, S.M., S.M.-S., E.M.G.F., R.D.S.; Visualization, V.F.A., S.M.-S.; supervision, S.M. and S.M.-S.; funding acquisition, V.F.A., S.M., S.M.-S., E.M.G.F. and R.D.S. All authors have read and agreed to the published version of the manuscript.

Funding: This work was partially supported by RNP, with resources from MCTIC, Grant No. 01245.010604/2020-14, under the Brazil 6G project of the Radiocommunication Reference Center (Centro de Referência em Radiocomunicações—CRR) of the National Institute of Telecommunications (Instituto Nacional de Telecomunicações—Inatel), Brazil, the National Council for Scientific and Technological Development-CNPq (403827/2021-3, 305021/2021-4), FAPESP (2021/06946-0), and by FONDECYT Iniciación No. 11200659 "Toward High Performance Wireless Connectivity for IoT and Beyond-5G Networks" in Chile.

Institutional Review Board Statement: Not applicable.

Informed Consent Statement: Not applicable.

Data Availability Statement: Not applicable.

Conflicts of Interest: The authors declare no conflict of interest.

Abbreviations

The following abbreviations are used in this manuscript:

AWGN	Additive White Gaussian Noise
BNC	Bit Layer Network Coding
BSI	Buffer State Information
CC	Cooperative Communication
CSI	Channel State Information
FD	Full Duplex
FIFO	First-In, First-Out
MC	Markov Chain
NOMA	Non-Orthogonal Multiple Access
OP	Outage Probability
PNC	Physical-layer Network Coding
TDBC	Time Division Broadcast
TWRN	Two-Way Relaying Network
iid	Independent and Identically Distributed
SNR	Signal-to-Noise Ratio

References

1. Verma, P.K.; Verma, R.; Prakash, A.; Agrawal, A.; Naik, K.; Tripathi, R.; Alsabaan, M.; Khalifa, T.; Abdelkader, T.; Abogharaf, A. Machine-to-Machine (M2M) communications: A survey. *J. Netw. Comput. Appl.* **2016**, *66*, 83–105. [CrossRef]
2. Ali, A.; Shah, G.A.; Farooq, M.O.; Ghani, U. Technologies and challenges in developing Machine-to-Machine applications: A survey. *J. Netw. Comput. Appl.* **2017**, *83*, 124–139. [CrossRef]
3. Andreev, S.; Galinina, O.; Pyattaev, A.; Gerasimenko, M.; Tirronen, T.; Torsner, J.; Sachs, J.; Dohler, M.; Koucheryavy, Y. Understanding the IoT Connectivity Landscape: A Contemporary M2M Radio Technology Roadmap. *Commun. Mag. IEEE* **2015**, *53*, 32–40. [CrossRef]
4. Braud, T.; Chatzopoulos, D.H.P. Machine Type Communications in 6G. In *Computer Communications and Networks*; Springer: Berlin/Heidelberg, Germany, 2021. [CrossRef]
5. Zhou, Z.; Guo, Y.; He, Y.; Zhao, X.; Bazzi, W.M. Access Control and Resource Allocation for M2M Communications in Industrial Automation. *IEEE Trans. Ind. Inform.* **2019**, *15*, 3093–3103. [CrossRef]
6. Zheng, K.; Ou, S.; Alonso-Zarate, J.; Dohler, M.; Liu, F.; Zhu, H. Challenges of massive access in highly dense LTE-advanced networks with machine-to-machine communications. *IEEE Wirel. Commun.* **2014**, *21*, 12–18. [CrossRef]
7. Nikaein, N.; Krea, S. Latency for real-time machine-to-machine communication in LTE-based system architecture. In Proceedings of the 17th European Wireless 2011-Sustainable Wireless Technologies, Vienna, Austria, 27–29 April 2011; pp. 1–6.
8. Chen, K.C.; Lien, S.Y. Machine-to-machine communications: Technologies and challenges. *Ad Hoc Netw.* **2014**, *18*, 3–23. [CrossRef]
9. Ouni, R.; Saleem, K. Framework for Sustainable Wireless Sensor Network based Environmental Monitoring. *Sustainability* **2022**, *14*, 8356. [CrossRef]
10. Bae, J.; Lee, M.; Shin, C. A Data-based Fault-detection Model for Wireless Sensor Networks. *Sustainability* **2019**, *11*, 6171. [CrossRef]
11. Taneja, A.; Saluja, N.; Taneja, N.; Alqahtani, A.; Elmagzoub, M.A.; Shaikh, A.; Koundal, D. Power Optimization Model for Energy Sustainability in 6G Wireless Networks. *Sustainability* **2022**, *14*, 7310. [CrossRef]

12. Shehab, M.; Khattab, T.; Kucukvar, M.; Trinchero, D. The Role of 5G/6G Networks in Building Sustainable and Energy-Efficient Smart Cities. In Proceedings of the 2022 IEEE 7th International Energy Conference (ENERGYCON), Riga, Latvia, 9–12 May 2022; pp. 1–7. [CrossRef]
13. Abdollahi, A.; Rejeb, K.; Rejeb, A.; Mostafa, M.M.; Zailani, S. Wireless Sensor Networks in Agriculture: Insights from Bibliometric Analysis. *Sustainability* **2021**, *13*, 12011. [CrossRef]
14. Rodríguez-Robles, J.; Martin, Á.; Martin, S.; Ruipérez-Valiente, J.A.; Castro, M. Autonomous sensor network for rural agriculture environments, low cost, and energy self-charge. *Sustainability* **2020**, *12*, 5913. [CrossRef]
15. Imoize, A.L.; Obakhena, H.I.; Anyasi, F.I.; Sur, S.N. A Review of Energy Efficiency and Power Control Schemes in Ultra-Dense Cell-Free Massive MIMO Systems for Sustainable 6G Wireless Communication. *Sustainability* **2022**, *14*, 11100. [CrossRef]
16. Naseer, S.; Liu, W.; Sarkar, N.I.; Shafiq, M.; Choi, J.G. Smart City Taxi Trajectory Coverage and Capacity Evaluation Model for Vehicular Sensor Networks. *Sustainability* **2021**, *13*, 10907. [CrossRef]
17. Chen, Z.; Cai, L.X.; Cheng, Y.; Shan, H. Sustainable cooperative communication in wireless powered networks with energy harvesting relay. *IEEE Trans. Wirel. Commun.* **2017**, *16*, 8175–8189. [CrossRef]
18. Nosratinia, A.; Hunter, T.E.; Hedayat, A. Cooperative communication in wireless networks. *IEEE Commun. Mag.* **2004**, *13*, 74–80. [CrossRef]
19. Tao, X.; Xu, X.; Cui, Q. An overview of cooperative communications. *IEEE Commun. Mag.* **2012**, *50*, 65–71. [CrossRef]
20. Aishwarya, M.; Kirthiga, S. Relay assisted cooperative communication for wireless sensor networks. In Proceedings of the 2018 Second International Conference on Advances in Electronics, Computers and Communications (ICAECC), Bangalore, India, 9–10 February 2018; pp. 1–6. [CrossRef]
21. Rankov, B.; Wittneben, A. Spectral efficient protocols for half-duplex fading relay channels. *IEEE J. Sel. Areas Commun.* **2007**, *25*, 379–389. [CrossRef]
22. Tanoli, S.A.K.; Rehman, M.; Khan, M.B.; Jadoon, I.; Ali Khan, F.; Nawaz, F.; Shah, S.A.; Yang, X.; Nasir, A.A. An Experimental Channel Capacity Analysis of Cooperative Networks Using Universal Software Radio Peripheral (USRP). *Sustainability* **2018**, *10*, 1983. [CrossRef]
23. Cover, T.M.; Thomas, J.A. *Element of Information Theory*, 2nd ed.; Wiley: London, UK, 2006; Chapter 15, pp. 509–612.
24. Zlatanov, N.; Ikhlef, A.; Islam, T.; Schober, R. Buffer-aided cooperative communications: Opportunities and challenges. *IEEE Commun. Mag.* **2014**, *52*, 146–153. [CrossRef]
25. Arti, M.K. Two-Way Satellite Relaying with Estimated Channel Gains. *IEEE Trans. Commun.* **2016**, *64*, 2808–2820. [CrossRef]
26. Esli, C.; Wittneben, A. Multiuser MIMO two-way relaying for cellular communications. In Proceedings of the 2008 IEEE 19th International Symposium on Personal, Indoor and Mobile Radio Communications, Cannes, France, 15–18 September 2008; pp. 1–6. [CrossRef]
27. Chen, Z.; Kuehne, A.; Klein, A.; Loch, A.; Hollick, M.; Widmer, J. Two-way relaying for multiple applications in wireless sensor networks. In Proceedings of the 2012 International ITG Workshop on Smart Antennas (WSA), Dresden, Germany, 7–8 March 2012; pp. 318–324. [CrossRef]
28. Liu, P.; Kim, I. Performance Analysis of Bidirectional Communication Protocols Based on Decode-and-Forward Relaying. *IEEE Trans. Commun.* **2010**, *58*, 2683–2696. [CrossRef]
29. Kim, S.J.; Devroye, N.; Mitran, P.; Tarokh, V. Achievable Rate Regions and Performance Comparison of Half Duplex Bi-Directional Relaying Protocols. *IEEE Trans. Inf. Theory* **2011**, *57*, 6405–6418. [CrossRef]
30. Kim, S.J.; Mitran, P.; Tarokh, V. Performance Bounds for Bidirectional Coded Cooperation Protocols. *IEEE Trans. Inf. Theory* **2008**, *54*, 5235–5241. [CrossRef]
31. Pappas, N.; Ephremides, A.; Traganitis, A. Stability and performance issues of a relay assisted multiple access scheme with mpr capabilities. *Comput. Commun.* **2014**, *42*, 70–76. [CrossRef]
32. Pappas, N.; Kountouris, M.; Jeon, J.; Ephremides, A.; Traganitis, A. Effect of energy harvesting on stable throughput in cooperative relay systems. *J. Commun. Netw.* **2016**, *18*, 261–269. [CrossRef]
33. Ullah, U.; Khan, A.; Zareei, M.; Ali, I.; Khattak, H.A.; Din, I.U. Energy-Effective Cooperative and Reliable Delivery Routing Protocols for Underwater Wireless Sensor Networks. *Energies* **2019**, *12*, 2630. [CrossRef]
34. Jamali, V.; Zlatanov, N.; Schober, R. Bidirectional Buffer-Aided Relay Networks with Fixed Rate Transmission—Part II: Delay-Constrained Case. *IEEE Trans. Wirel. Commun.* **2015**, *14*, 1339–1355. [CrossRef]
35. Anyugu Francis Lin, B.; Ye, X.; Hao, S. Adaptive protocol for full-duplex two-way systems with the buffer-aided relaying. *IET Commun.* **2019**, *13*, 54–58. [CrossRef]
36. Lin, B.A.F. Throughput maximization for full-duplex two-way relay with finite buffers. *Indones. J. Electr. Eng. Comput. Sci.* **2020**, *20*, 854–862. [CrossRef]
37. Zhang, S.; Liew, S.C.; Lam, P.P. Hot topic: Physical-layer network coding. In Proceedings of the 12th Annual International Conference on Mobile Computing and Networking, Los Angeles, CA, USA, 23–29 September 2006; pp. 358–365.
38. Popovski, P.; Yomo, H. Physical network coding in two-way wireless relay channels. In Proceedings of the 2007 IEEE International Conference on Communications, Glasgow, UK, 24–28 June 2007; pp. 707–712.
39. Ni, W.; Zhang, J.A.; Fang, Z.; Abolhasan, M.; Liu, R.P.; Guo, Y.J. Analysis of Finite Buffer in Two-Way Relay: A Queueing Theoretic Point of View. *IEEE Trans. Veh. Technol.* **2018**, *67*, 3690–3694. [CrossRef]

40. Shi, S.; Li, S.; Tian, J. Markov Modeling for Practical Two-Way Relay with Finite Relay Buffer. *IEEE Commun. Lett.* **2016**, *20*, 768–771. [CrossRef]
41. Kumar, R.; Hossain, A. Performance of Random Access Markov Modelling for Two-Way Buffer-Aided Relaying Networks with Wireless Assisted Links. *Wirel. Pers. Commun.* **2019**, *108*, 1995–2015. [CrossRef]
42. Zhou, Q.F.; Zhao, L.; Peng, M.; Liu, X.; Fan, L. TDMA-Based Cooperative NC MAC Scheme for Two-Way Relaying Networks. *IEEE Access* **2018**, *6*, 7123–7133. [CrossRef]
43. Abou-Rjeily, C. Optimal Two-Way Buffer-Aided Relaying: Achieving the Best Outage and Delay Performance with Small Buffer Sizes. *IEEE Trans. Wirel. Commun.* **2021**, *20*, 2888–2901. [CrossRef]
44. Fang, Z.; Shen, S.; Liu, J.; Ni, W.; Jamalipour, A. New NOMA-Based Two-Way Relay Networks. *IEEE Trans. Veh. Technol.* **2020**, *69*, 15314–15324. [CrossRef]
45. El-Rajab, M.; Abou-Rjeily, C.; Kfouri, R. Buffer-aided relaying: A survey on relay selection policies. *IET Commun.* **2020**, *14*, 3715–3734. [CrossRef]
46. Jamali, V.; Zlatanov, N.; Schober, R. Bidirectional Buffer-Aided Relay Networks with Fixed Rate Transmission—Part I: Delay-Unconstrained Case. *IEEE Trans. Wirel. Commun.* **2015**, *14*, 1323–1338. [CrossRef]
47. Shi, S.; Li, S.; Tian, J. Performance Analysis for Practical XOR Two-Way Relay under Finite Relay Buffer. *Int. J. Wirel. Inf. Netw.* **2016**, *23*, 112–121. [CrossRef]
48. Phan, K.T.; Le-Ngoc, T.; Le, L.B. Optimal Resource Allocation for Buffer-Aided Relaying with Statistical QoS Constraint. *IEEE Trans. Commun.* **2016**, *64*, 959–972. [CrossRef]
49. Phan, K.T.; Huynh, P.; Nguyen, D.N.; Ngo, D.T.; Hong, Y.; Le-Ngoc, T. Energy-Efficient Dual-Hop Internet of Things Communications Network with Delay-Outage Constraints. *IEEE Trans. Ind. Inform.* **2021**, *17*, 4892–4903. [CrossRef]
50. Arshad, S.A.; Murtaza, M.; Tahir, M. Optimal buffer management for relay nodes in integrated wireless sensor and vehicular networks. In Proceedings of the 2012 IEEE Consumer Communications and Networking Conference (CCNC), Las Vegas, NV, USA, 14–17 January 2012; pp. 366–367. [CrossRef]
51. Bletsas, A.; Khisti, A.; Reed, D.; Lippman, A. A simple Cooperative diversity method based on network path selection. *IEEE J. Sel. Areas Commun.* **2006**, *24*, 659–672. [CrossRef]
52. Zhou, Q.F.; Li, Y.; Lau, F.C.M.; Vucetic, B. Decode-and-Forward Two-Way Relaying with Network Coding and Opportunistic Relay Selection. *IEEE Trans. Commun.* **2010**, *58*, 3070–3076. [CrossRef]
53. Ahlswede, R.; Cai, N.; Li, S.Y.; Yeung, R. Network information flow. *IEEE Trans. Inf. Theory* **2000**, *46*, 1204–1216. [CrossRef]
54. Liu, H.; Popovski, P.; de Carvalho, E.; Zhao, Y. Sum-Rate Optimization in a Two-Way Relay Network with Buffering. *IEEE Commun. Lett.* **2013**, *17*, 95–98. [CrossRef]
55. Goldsmith, A. Capacity of Wireless Channels. In *Wireless Communications*; Cambridge University Press: New York, NY, USA, 2005; Chapter 4, pp. 99–125.
56. Louie, R.H.; Li, Y.; Vucetic, B. Practical physical layer network coding for two-way relay channels: Performance analysis and comparison. *IEEE Trans. Wirel. Commun.* **2010**, *9*, 764–777. [CrossRef]
57. Kim, S.J.; Mitran, P.; John, C.; Ghanadan, R.; Tarokh, V. Coded bi-directional relaying in combat scenarios. In Proceedings of the MILCOM 2007—IEEE Military Communications Conference, Orlando, FL, USA, 29–31 October 2007; pp. 1–7. [CrossRef]
58. Minhas, H.I.; Ahmad, R.; Ahmed, W.; Waheed, M.; Alam, M.M.; Gul, S.T. A reinforcement learning routing protocol for UAV aided public safety networks. *Sensors* **2021**, *21*, 4121. [CrossRef] [PubMed]
59. Huang, J.; Gharavi, H. Performance Analysis of Relay-Based Two-Way D2D Communications with Network Coding. *IEEE Trans. Veh. Technol.* **2018**, *67*, 6642–6646. [CrossRef]
60. Adanvo, V.F. Buffer-Aided-Relaying-Strategies-Two-Way-Wireless-Networks. GitHub Repository. Available online: https://github.com/Vignonfidele/Buffer-Aided-Relaying-Strategies-Two-Way-Wireless-Networks.git (accessed on 20 September 2022).